Biosorption of Heavy Metal and Organic Dyes from Textile Wastewater using Algal Derived Biochar

By

Abdul Ahad Khan

School of Chemical and Materials Engineering

National University of Sciences and Technology

2022

Biosorption of Heavy Metal and Organic Dyes from Textile Wastewater using Algal Derived Biochar

Name: Abdul Ahad Khan

Registration No: 00000327370

This thesis is submitted as a partial fulfillment of the requirements for the degree of

MS in Chemical Engineering

Supervisor Name: Dr. Salman Raza Naqvi

School of Chemical and Materials Engineering (SCME)

National University of Science and Technology (NUST)

H-12, Islamabad, Pakistan.

Dedication

By the grace of Almighty Allah, who is the most Beneficent and the most merciful

This research is dedicated to my parents, who have always been my source of guidance and support.

To my supervisor who shared his knowledge, gave advice, and encouraged me to fulfill my tasks.

And to all my fellows, with whom I worked with and shared good memories.

Acknowledgements

Abstract

Textile industries release effluent that contains the vast majority of heavy metals and dyes in which Cr (VI) and Congo red Dye is a toxic carcinogenic element that causes an environmental problem. The work aims to synthesize algal-derived biochar using slow pyrolysis at an operating temperature of 500 °C, a heating rate of 10 °C/min and a residence time of 60 min and use it as an adsorbent to remove Cr (VI) and Congo red Dye. The batch experiment was carried out using different concentrations of Cr (VI) and Congo red Dye (1, 10, 25, 50, 100, 125, 150 and 200 ppm) at different intervals of time (2.5, 5, 10, 15, 30, 60, 120 and 240 min). The maximum removal percentage of Cr (VI) is 97.88 % and Congo Red Dye is 96.14029 % for the metal concentration of 1 ppm exhibiting non-linear adsorption isotherm (Langmuir, Freundlich, Dubinin-Radushkevich, and Temkin models) and kinetic models (pseudo-first order, pseudo-second order, nth order, and intra-particular diffusion) were analyzed using a solver add-in of Microsoft Excel. According to the results, the Langmuir isotherm model (R^2 = 0.999, R^2=0.996) and pseudo-nth order models are suitable to describe the monolayer adsorption and the process kinetics, respectively. The maximum adsorption capacity of algal biochar to adsorb is 186.94 mg/g for Cr (VI) and 179.9524 mg/g for Congo red Dye. For the prediction of optimal removal efficacy, an artificial neural network of the MLP-2-7-1 (Cr (VI) and MLP-2-5-1(Congo Red Dye) model was used. The results obtained are useful for future work using algal biochar as an adsorbent of Cr (VI) and Congo Red Dye from textile wastewater to achieve sustainable development goals.

Table of Contents

List of Figure

List of Table

Acronym

IUPAC: International Union of Pure and Applied Chemistry

IARC: International Agency for Research on Cancer

WHO: World Health Organization

BOD: Biological Oxygen Demand

COD   Chemical Oxygen Demand

HTC   Hydrothermal Carbonization

NIOSH   National Institute of Occupational Safety and Health

NOCs   Non-biodegradable Organic Compounds

TDS   Total Dissolved Solids

pH   Potential of Hydrogen

PFO: Pseudo First Order

PSO: Pseudo Second Order

PNO: Pseudo nth Order

SEM: Scanning Electron Microscope

EDX: Energy Dispersive X-ray Spectroscopy

FTIR: Fourier Transform Infrared Radiation

D-R: Dubinin-Radushkevish

Chapter 1

Introduction

1.1 Background

Water resources worldwide are being unusable due to the discharge of inorganic and organic contaminants such as heavy metals, dyes, and unwanted products from industries into water bodies[1]. Heavy metals have an adverse effect on human health and aquatic ecosystems, making water pollution a global environmental problem [2]. Various industries (i.e., leather, dye, fertilizer, etc.) release wastewater in which the textile industry releases a substantial amount of effluents containing various harmful constituents, such as dyes, various chemicals, and heavy metals into water resources every year, creating serious environmental problems [3] Untreated dyes are present in significant amounts in industrial wastewater. The residual dye is an organic pollutant coming from different sources, such as textiles, paper, pulp, and pharmaceutical industries[4].The textile industry uses a lot of dye to color its goods. Effluent containing the dye is discharged into the wastewater alongside heavy metals that are essential to the dye's composition. Traditional wastewater treatment methods (coagulation, membrane technology, electrolysis ion exchange, and so on) are costly and inefficient when used to textile industry wastewater (. Additionally, most of these methods result in toxic sludge, making them harmful to the environment. The food, beauty, and energy sectors are all seeing growth in the algae-based economy. As a result of the different functional groups present on its surface and the presence of different cations, algae biomass is distinct from lignocellulosic biomass. As a decontamination method, biochar is unparalleled due to these two features. Organic pollutants (dyes) and heavy metals may be effectively removed using the functional groups and cations found in algae biomass. Microalgae and macroalgae are two types of algae with vastly varied biomass compositions, which means they will both produce distinct biochar even when subjected to the identical synthesis conditions. New sustainable

and cost-effective methods for treating wastewater from the textile industry have been developed using absorbents produced from algal biomass. Microalgal biochar was used in a biosorption process to remove organic contaminants (dyes) and heavy metals from textile effluents. In this article, we'll look at adsorbing dyes and metal pollutant as well as the various processes for generating algal biochar (pyrolysis, hydrothermal carbonization, and torrefaction). There hasn't been much research done on microalgal biomass for biochar using hydrothermal carbonization and torrefaction. Similar to lignocellulosic biomass, biochar undergoes significant structural and functional group modifications when compared to the original microalgal biomass.

1.2 Textile effluents:

The textile industry is a major consumer of water, with much of that water ending up in the environment as effluent. The percentage of various sorts of industries' effluent that contains dyes and is discharged into local waterways shows in Fig. 1. The wastewater generated by the textile industry is the principal source of pollution since it contains significant volumes of a wide variety of dyes. During the dying process, between ten and twenty-five percent of the textile dye is lost, and an additional eleven to sixteen percent of the dye ends up in the wastewater
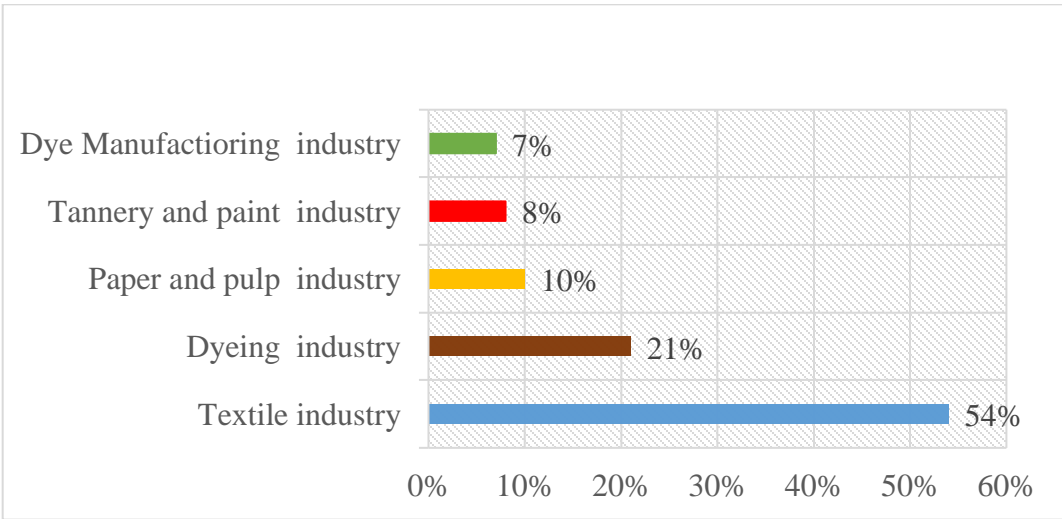
Figure 1: Contribution of different industries to discharge of dye-containing wastewater.

2

Studies on biochar–dye interaction will be important, as the problem of dye contamination in water is growing in most of countries worldwide. Textile wastewater is classified according to its color, salinity, temperature, pH, BOD, COD, Total phosphorus, TDS, nitrogen, and NOCs[5]. Wastewater from the textile industry often contains heavy metals used in the dyeing process, i.e., chromium (Cr), arsenic (As), etc. The composition of the wastewater from textile industry varies among factories and countries, based on the manufacturing process, type of fabric synthesis, and factory equipment used which shown in Fig. 2 [6]. Pollutants released into the environment without any form of regulation pose the greatest threat to the health of the planet's ecosystems. [7].
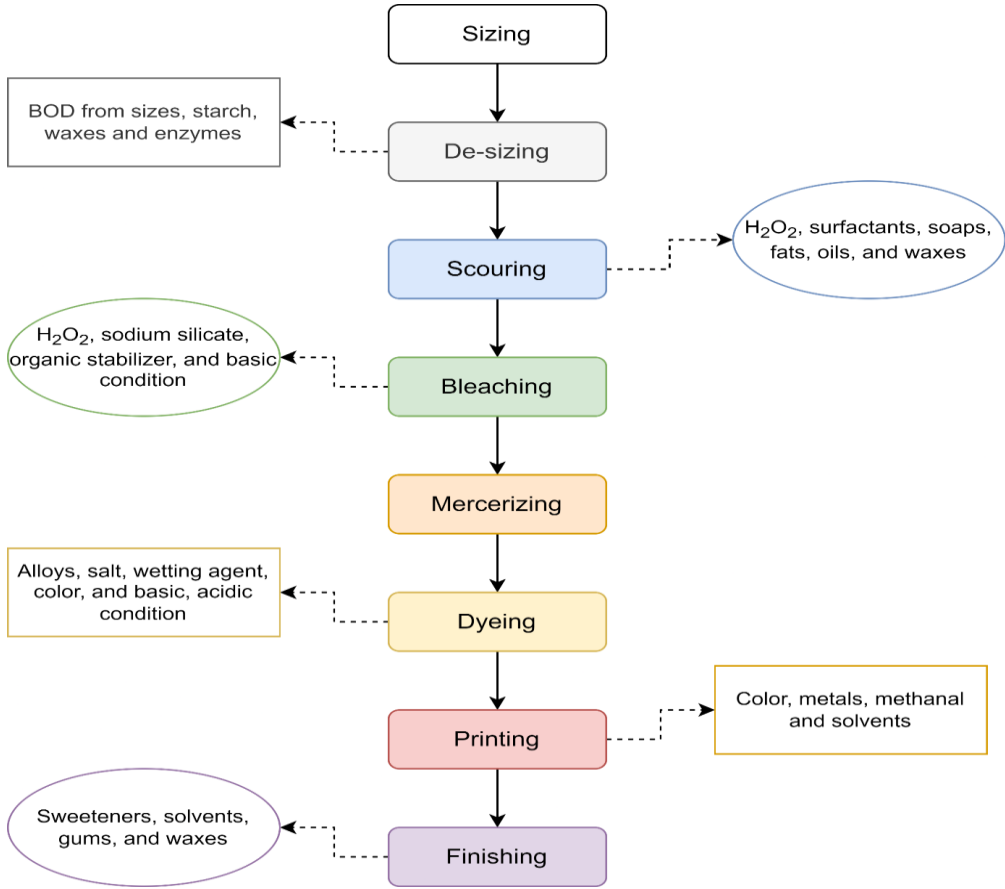
Figure 2: Extraction of metal and color dye wastes in processes of the textile.

1.3 Organic Pollutant of textile Industry

As a result of their xenobiotic nature, textile dyes are aromatic synthetic chemical compounds that are resistant to biodegradation. Dye (soluble organic compound) is a molecule comprising two chemical groups, one is a chromophore (give color), and the other is auxochrome (fix dye molecule in the tissue)[8]. Classification of different dyes are shown in Fig. 3[9]. Textile dye is a toxic and carcinogenic agent. It causes aesthetic damage to water bodies and prevents light from reaching the water, and causes a decrease in the rate of photosynthesis.

Methylene blue

It is found in a considerable amount of textile effluent. Methylene blue exposure can cause various health issues such as headaches, vomiting, disorientation, shortness of breath, and elevated blood pressure. Additionally, serotonin syndrome, red blood cell disintegration, and allergic reactions can occur[10].

Azo dyes

This dye appears to be the most frequently utilized synthetic color in the apparel industry and may be present in substantial amounts in wastewater. Azoic dyes are highly used in dye industries, and their use may expand in the future. They have a significant impact on the dyeing and printing sectors. Azoic dyes are the most deleterious types of synthetic dye present in textile industry effluents due to their chemical structure, which contains azoic linkages, amino groups, and aromatic rings. They appear to be extremely resilient within aquatic ecosystems. Uncontrolled discharge of azo dyes into bodies of water creates major environmental problems, including decreased light absorption and the formation of various amines under anaerobic conditions[11]. There are many types of azoic dyes, which are described below.

Direct blue 15

In the textile industry, a colorant based on dimethoxy benzidine is utilised to address mutagenesis issues. [12].

Acid violet 7

This dye is used in various sectors such as food, paper, paint, and, most notably, textiles. The harmful effect of this dye is a chromosomal abnormality, suppression of acetylcholinesterase activity, and peroxidation of membrane lipids[13].

Cationic dyes

Cationic polymer dyes typically create ionic connections with the dyes used on these substrates. Because polyamides such as nylon and proteins such as wool, silk, and leather contain a positive charge (cationic), anionic dyes are employed in this application. Acid dyes, such as C.I. Acid Black 1, are anionic dyes that are compatible with polyamide and protein substrates. These dyes are toxic colorants that cause allergic reactions, cancer, and mutagen diseases.

Disperse dyes

Disperse dyes are the name given to the type of dye produced specifically for polyester. The dye is "dissolved" in the polymer matrix, resulting in a solid-solid solution in this example. As a result of the well-known "like dissolves like" concept, hydrophobic disperse dyes are designed. It is because they are scattered in water rather than dissolved in water that they are known as dispersible dyes. C.I. Disperse Blue 165 is one such example.
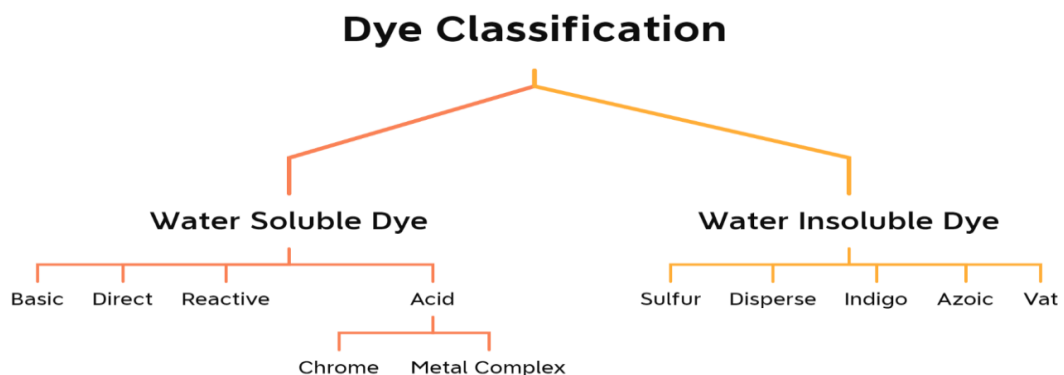
Figure 3: Classification of dyes

1.4 Congo Red Dye

Congo red, also known as 3,3′-([1,1′-biphenyl]-4,4′-diyl) bis (NaOH), is a chemical compound (4-aminonaphthalene-1-sulfonic acid). Specifically, it is an azo dye. Even though Congo red can be dissolved in water to make a red colloidal solution, it is more soluble in organic solvents. Synthetic colorants such as azo dyes (Congo red) are widely used in the textile industry because of their many advantages. These include their low energy consumption, excellent resistance to fading, and extensive colour palette. In azo dyes, the quantity of chromophoric groups and aromatic rings can vary. The -conjugated azo link and its resonance make azo dyes extremely stable and useful in a wide variety of industries, including the chemical, textile, paper, cosmetic, and pharmaceutical industries. The world produces up to 108 metric tonnes of dyes annually, with azo dyes making up between sixty and seventy percent of the total. The overuse of azo dyes causes massive volumes of wastewater pollution. Congo Red (diazo dye) is considered to be carcinogenic due to the presence of an aromatic amine in its chemical composition[14]. Due of their aromatic qualities, azo dyes are resistant to degradation in the natural world. Dye exposure causes illness and death in a wide variety of animal and plant species because the dyes remain in the environment for extended periods of time8. Therefore, it is crucial to remove the Congo Red dye from the polluted water.

1.5 Heavy metals in textile effluent

Metal ions are included in a dye structure to create a bathochromic shift resulting in an excellent coloration. Heavy metals consist of essential (Zn, Fe, Ni, Cu) and non-essential (Cd, Hg, Pb, As, and Sn) metals with atomic number >23 and are water-soluble[15]. Heavy metals (Cu, Fe, Mn, Ba &Pb) metals are part of vat dyes due to their production process. Heavy metals are released from textile industry during the process of pre-treatment, dyeing, printing and finishing steps due to the utilization of chemicals and complex dyes that contain metals. For example, a large number of chemicals can be utilized during textile processing such as, metal complex dyes, oxidizing agents, chemicals from the catalyst, getting bright dark colors chrome or mordant dyes and fixing agent

cross-linking agent etc. Because of their complicated molecular structure, heavy metals with a density more than 5 mg per cubic centimeter are non-biodegradable and more difficult to remove. The most common metal ions that are discharge from textile industry and found in textile effluents are Cd (II), Cr (VI), Zn (II) and Pb (II). Chromium (Cr) become part of textile wastewater as dichromate of chromate salt during the dyeing process for dye fixation during printing with printing paste chromium (III). Moreover, unfixed dyes are also the source of heavy metals contamination[16].

The high toxicity and carcinogenicity of heavy metals cause negative effects on wildlife, agriculture, the marine environment, and humans. [17]. Color pigments for textile dyes are commonly produced using heavy metals such as lead (Pb), chromium (Cr), cadmium (Cd), copper (Cu), and nickel (Ni). The level of toxicity of several selected metals for humans is as follows[18]:

$$Co < Al < Cr < Pb < Ni < Zn < Cu < Cd$$

Heavy metals such as chromium, lead, and cadmium are released into the textile effluent, so it is necessary to eliminate this harmful metal. The contamination of heavy metals existing in water is one of the leading sources of serious diseases and death.

Cadmium chloride is used during dying process, Cd is a poisonous substance and can even cause cancer and premature death; long-term acquaintance to Cd leads to systemic toxicity in the reproductive, skeletal, urinary, respiratory, and nervous systems[19, 20]. The minimum concentration in wastewater recommended by WHO is 0.03 mg/l[21].

Disease like endocrine, neurological, circulatory, skeletal, and immune systems are all harmed by lead (Pb), which can also impair a child's brain development. Additionally, it is extremely damaging to plants, causing severe damage to the chlorophyll and resulting growth inhibition.[22]. The allowable level of lead in wastewater is 0.01 mg/l[21].

Zinc (Zn) is another heavy metal and is required for the proper function of the human body, unlike Cd and Pb. Although Zn is an essential element for the human body, long-term exposure to the excess amount of Zn causes infertility and decreases immune

function and cholesterol balance. Cd, Pb, and Zn also accumulate in crops and vegetables in fields near polluted areas.

Nickel (Ni) is omnipresent, but its role in animal life has not yet been clearly understood. Exposure to Ni can cause lung fibrosis, allergy, kidney disease, cardiovascular disease and lead to cancer and epigenetic changes[23]. The safe level of nickel in wastewater is 0.02 mg/l.

1.6 Chromium

Chromium (Cr) a metallic element that is present in trace amounts in the earth's crust. Numerous significant alloys have chromium as the primary element. Chromium has been identified as one of the toxic carcinogenic elements found in textile effluent. According to the latest IUPAC periodic table, chromium is the sixth group element present in the environment, having an oxidation state ranging from -2 to +6[24], however, the most stable forms are Cr (III) and Cr (VI) [25]. Cr (VI) is 100 times more harmful than Cr (III) according to the IARC report [26]. The major target organ for chromium toxicity (VI) is the respiratory tract, which causes chronic and acute exposure to inhalation. Inhalation of Cr (VI) causes lung tumors in animals and increases the risk of lung cancer in humans. Hexavalent chromium also has other various health detriments, i.e., nosocomial, kidney disease, liver problems, chromosomic aberrations, and dermatitis [27] Chromium pollution occurs as a result of industrial and agricultural activities. Chromium has a wide range of industrial applications, including alloying, pulp, and paper manufacturing. Chromium is a trace element that is required in drinking water by most animals, including humans, for blood vessel function and iron metabolism. Factory workers exposed to chromium dust have reported experiencing eye inflammation. In addition, it is becoming more prevalent in oil well drilling, tanneries, and metal plating. Exposure to Cr (VI) causes cancer of the digestive system and lungs, as well as epigastric discomfort and hemorrhage. According to WHO, the allowable limit of chromium in wastewater is 0.05 mg/l[21].

1.7 Algae

Algae contain hydrocarbon, which are influenced by a number of variables, including temperature, pH, salinity, light intensity, and nutrition availability (K, N, P, etc.)[28]. Microalgae have the fine particle structure which contain no low lignin content. This is related to their fats, ash, water and protein content as comparted to the lignocellulosic biomass. Due to the particle structure and constituents this low lignin microalgae can be treated by simpler pretreatment methods. Lignocellulosic biomass has a complex fibrous structure which requires complex treatment methods to achieve desirable biochar. Due to the nature of microalgae, biochar is one of the useful uses with a sustainable supply of raw materials. [29]. Adsorbents with desirable qualities including porosity, stability, insolubility, and aromaticity can be made using microalgae biochar. After those steps are taken, biochar can be effectively used to treat wastewater. Bioremediation of agro-industrial waste water using microalgal biochar has been shown to be effective at removing heavy metals and dyes.[30].

1.8 Biochar

Biochar is a carbon-based material that has gained popularity in recent years due to the positive potential in environmental management. It is a solid biomass product with a high carbon content (65–90%), a porous structure, and an oxygen functional group-containing surface. It is an item that was produced using biomass. [31].

1.9 Problem Statement

Removal of Cr (VI) and Congo Red Dye from Textile Waste water using the conventional method have many limitations such as high cost of operation and maintenance, the consumption of chemicals, the energy used, the inefficiency to remove pollutants present in very low concentrations, and the complexity of the process. To reduce this limitation, develop a biosorption technique such as algal derived biochar possess high affinity for adsorption and electrostatic removal of these pollutant.

1.10 Research Objective

The research objective is as follow

- Biochar synthesis using algae as feedstock through slow pyrolysis (500 ℃).
- Determine the removal efficacy and adsorption capacity by changing the concentration of hexavalent chromium and Congo Red Dye at different intervals of time.
- Study the non-linear adsorption isotherm and the kinetic model and determine which model is the best fit to describe the adsorption behavior and mechanism.
- Determine the best fit model to predict the target value of removal efficacy and kinetics of Cr (VI) and Congo Red Dye using the ANN model.
- Characterize the algae, biochar and Cr (VI) and Congo Red Dye loaded biochar using SEM and FTIR.

1.11 Scope of Study

Pakistan, once a water-surplus country, is now a water deficit country. The water availability has decreased from 1,299 m³ per capita in 1996-97 to 1,100 m³ per capita in 2006 and it is projected to less than 700 m³ per capita by 2025. In Pakistan only 1% of the domestic and industrial wastewater receives treatment. To overcome the shortage of wastewater it is necessary to treat the industrial wastewater so that to reuse the water again and make the Pakistan water excess country

- The project is important due to utilizing of biochar, which is stable in the environment, has well-developed pores, and is biocompatible. It is also a low-cost, highly efficient adsorbent with a lot of potential for getting rid of pollutants.
- The main significance of project is water purification using renewable, promising and sustainable feedstock

1.12 Chapter Summary

This thesis consists of five chapters. The acquaintance of each chapter is given in the following chapters.

- **Chapter 1** delivers vision of the subject, background and contemporary problems related to the work. It also clarifies the problem statement, research objectives and scope of the planned study.

- **Chapter 2** will sketch the literature review achieved to describe the previous work done on the synthesis of biochar, previous method technique, Biosorption through microalgal biochar its factors. It also includes review based to compare algal biomass with different biomass.

- **Chapter 3** covers the methodology related to the synthesis of biochar, preparation of stock solution. This study includes the non-linear isotherm and kinetics model. The study about Artificial Neural Network and characterization of algae, biochar before and after adsorption also the part of this chapter.

- **Chapter 4** elaborate the result and discussion. The analysis of isotherm and kinetics model to describe the adsorption mechanism and tell us which model is best for the removal of pollutants on the surface of algal biochar. The chapter also elaborate the result of ANN model and characterization of algal biochar before and after adsorption.

- **Chapter 5** reviews all the findings and conclusions in the current study and provides the future recommendation for the related work.

Chapter 2

Literature Review

2.1 Literature Review

Algae is multifunctional characteristics, including as energy production, algae have garnered a great deal of study interest.[32], wastewater treatment[33], and carbon dioxide emission[34]. Proteins, lipids, and carbohydrates are the primary chemical components of algal biomass, but their relative composition varies among algal species.[35]. The rate of growth of algae is 5- 10 times that of terrestrial plants. Due of their photosynthetic capabilities, algae are promising for biotreatment. Algae are intriguing due to their ability to assimilate these compounds and use them as a carbon source [36, 37].

Various strains of Algae are selected for their ability to remove hazardous materials from wastewater, such as Scenedesmus obliquus (to remove benzophenone in water), *Oscillatoria* sp., and *Chlorella* sp. (to remove dyes from wastewater through biosorption[38] . Algal biochar is used for energy storage and adsorption by creating strategies to expand its porous structure or by synthesizing algal base porous carbon, according to the literature and contemporary research.[39]. Different chemical reagent (Zinc chloride, Potassium Per magnate) is used in recent work for the modification of algal biochar. This modified biochar is used for enhancement of adsorption of heavy metal such as cadmium from waste water[40]..Other than biomass, metabolites such as lipids or carbohydrate extracted biomass will offer a biochar with its unique characteristics. Variation in Algae species and their growth environment is expected to play a major role in the properties of resultant biochar. This review summarizes and evaluate the possibility of using Algae biomass and biochar for textile waste water treatment to remove heavy metals and organic dyes. This review also aims to high light the importance of important characteristic of biochar that are essentials for its use as environmental remediation agent. A future recommendation of research work related to algal biochar is also proposed in the review. This review highlights the progress made Algae-derived biochar to treat textile

industry wastewater, along with the selection of methods for its preparation, as per intended use of biochar from Algae.

2.2 Algae and Types:

Algae are unicellular microscopic organisms have the fine particle structure which contain no low lignin content [41]. This is related to their fats, ash, water and protein content as comparted to the lignocellulosic biomass. Due to the particle structure and constituents this low lignin Algae can be treated by simpler pretreatment methods. Lignocellulosic biomass have a complex fibrous structure which requires complex treatment methods to achieve desirable biochar[42]. Other advantages of algal biomass include lower soil requirements, higher yields, and a broad range for aquatic habitats. These essential characteristics pertain to the examination of algae for potential applications such as wastewater treatment.,[42] biofuels, health supplements, cosmetics and pharmaceuticals[41]. Biochar is one of the promising applications with a sustainable raw material supply due to the characteristics of algae[29]. The remarkable qualities of porosity, stability, insolubility, and aromaticity can be cultivated in adsorbents by using algae biochar. Once the biochar is made, it can be put to good use in cleaning polluted water. Bioremediation of agro-industrial waste water can follow the use of algae charcoal to remove heavy metals and dyes.[30].

According to various types of metabolic modes Algae are also classified. These metabolic modes are mixotrophic, heterotrophic, and phototrophic. Studied have been shown that 40,000 various species of Algae are present[28]. Different Algae are present which have good capacity of adsorption such as Chlorella vulgaris, Chlamydomonas and Desmodesmus etc. Various Algae are used for the adsorption of heavy metal and dyes from wastewater such as Sargassum, Lyngbya taylorii, green algae (Chlorella, and diatoms such as Phaeodactylum, Cyclotella and Aulosira as well as cyanobacteria such as Spirulina, Oscillatoria and Phormidium autumnale UTEX1580), Parachlorella sp. ,Oedogonium sp. , multivariabilis, m Spirulina platensis Microspora sp., Ulothrix zonata, Spirulina platensis and Cosmarium sp [30].

2.3 Biochar production from Algae by the thermochemical method

The common method for the production of biochar is thermochemical conversion, including hydrothermal carbonization, Pyrolysis, gasification, and torrefaction[43]. For the high production of biochar, the process method must be appropriate for biomass use, and the process factors (residence time, temperature, and heating rate) must be optimal. These parameters are critical because they can have an effect on the chemical and physical states of biochar during the manufacturing process[1]. The thermochemical conversion to produce biochar are illustrate in Table. 1. The biomass elaborate in this review is Algae.

Table 1: Thermochemical conversion of Algae for the synthesis of biochar

Biomass Source	Type of Processes	Temp (°C)	Biochar yield (%)	Ref
Dunaliella tertiolecta	Slow Pyrolysis	500	63	[42]
Chlorella protothecoides	Fast Pyrolysis	500	54	[44]
Spirulina	Microwave assisted Pyrolysis	400-700	5.1-9.6	[42]
Pavlava	Catalytical Pyrolysis	500	36-47	[45]
Nannochloropsis	Catalytic (HZMS-5 zeolite)	500	21.7	[46]

	Pyrolysis			
Oscillatoria	Catalytic (TiO$_2$ & ZnO) Pyrolysis	550	53.05	[47]
Chlorella sp. G.D.	Wet torrefaction	160 -170	74.8	[48]
Chlorella vulgaris FSP-E (high protein) with microwave	Wet Torrefaction	160	64.20–66.90	[49]
Chlorella sorokiniana CY1	Dry Torrefaction	200	85.76	[42]
Chlamydomonas reinhardtii	Hydrothermal carbonization	200	39	[50]
Synechocysti sp.	Hydrothermal carbonization	213	18	[50]

2.3.1 Pyrolysis

Pyrolysis is the thermal degradation of organic compounds in the absence of oxygen at temperatures between 523.15 - 1173.15 K[51]. According to retention time, temperature, heating rate, and pressure, pyrolysis is primarily categorized as rapid, ultrafast, ash, and slow pyrolysis. The temperature affects the product's effectiveness; raising the temperature reduces the biochar yield.[52, 53]. Slow Pyrolysis produces a finer biochar yield differentiating to fast Pyrolysis shown in Table. 1. In brief, 50.0 g of Algae produce biochar in the range of 68 -74 at various pyrolysis temperatures. Air-dried algal biomass was sieved (0.25 mm) into crucibles sealed with lids to keep oxygen out and Pyrolysis in a muffle furnace prior to charring. An empty metal drum was perforated on the sides (approximately mm), and a 30 cm diameter aperture was built on top of the container to

assist the arrangement of fuelwood for burning in the muffle furnace. The bottom of the drum was completely removed. To facilitate charring, a fire was ignited in the container. The algal biomass was burned into carbonated algal biomass as the heat was passed through the perforated holes. Using a semi-indirect heating approach, the algal biomass was slowly pyrolyzed in the pyrolysis unit at temperatures of 350-600 °C. In recent findings, dried algal biomass (500 g) was placed in the container at different temperatures (such as 350, 400, 450, 500, 550, and 600 °C) for 1 hour for the production of biochar[54]. The percentage of oil and gas at discussed temperatures was 42.6, 47.6, 38, 44, 36, and 32%. The biochar obtained from Chlorella sp. residue through Pyrolysis has a high surface area($266 \ m^2/g$) as compared to other thermochemical methods using variant Algae[55].

2.3.2 Hydrothermal carbonization

HTC is a relatively innovative and intriguing thermochemical process that uses microalgal biomass to produce biochar. Biomass having elevated moisture content converted directly into the carbon-rich solid material term hydro char. Generally, this approach heats the biomasses of most microalgal species in the aqueous medium to a temperature range between 448 and 523 K during a reaction time (0.5 to 20 h) at a pressure of 2000 to 6000 kPa. For example, Algae such as Nannochloropsis *sp.,* Spirulina produce biochar through the process of hydrothermal carbonization. HTC enables the exclusion of external and internal moisture from the biomass and helps to pressurize the reactor, and this is done at a lower temperature. Thus, the method by which hydrochar is produced is distinct from the mechanism by which Pyrolysis occurs. HTC begins with the breakdown of hemicellulose and cellulose, and the polymerization of the intermediate results in the formation of hydrochars[56, 57]. The first step of hydrothermal carbonization of Algae is pretreatment, where washing, drying, and grinding is occurred. After the pretreatment of Algae, it enters into the hydrothermal carbonization process in a tube furnace where three products is obtained gas, solid (main product), and liquid. Hydrothermal carbonization enhances the oxygen-containing functional group of Algae-derived biochar. This method also affects the surface area of biochar, such as the surface area of Spirulina sp. is 96.5 m^2/g[58].

2.3.3 Torrefaction

Torrefaction is a relatively new thermochemical conversion process that is used to extract volatiles from microalgal biomass. Torrefaction are classified as dry or moist. Dry torrefaction is different from wet torrefaction. Dry torrefaction under anaerobic conditions occurs at a temperature (473 - 573 K) and atmospheric pressure to heat biomass and uses inert nitrogen gas. However, wet torrefaction uses hot compressed water, a temperature range (453 - 533 K), and a shorter residence time (5 min) to heat biomass. The wet torrefaction synthesizes solid products with high energy density, hydrophobicity, and lower ash content compared to that of dry torrefaction, but both have a major effect on the absorptivity of biochar. Because of faster heat transfer, the decomposition of raw wet microalgal biomass via hydrolysis attack is easy than the dry torrefaction making wet torrefaction a more promising pretreatment method. However, wet torrefaction has a number of disadvantages, including the fact that high pressure causes high maintenance and setup costs, upgrading microalgal biomass that has a high moisture content requires high energy requirements, and the addition of solid product extraction methods (such as filtration and evaporation). Dry torrefaction produces more biochar (solid) than wet torrefaction, which has received little research on its efficacy in converting biomass to biochar. The result indicates that dry torrefaction produced more solid at a lower temperature. Torrefaction studies with various species of Algae are summarized in Table In general, a low-temperature torrefaction procedure with a short residence period and a low heating rate results in increased biochar production[57]. Furthermore, torrefaction enhances the synthesis of hydrophobic biochar due to the destruction and removal of -O.H. groups in microalgal biomass during the heating process[59, 60]. The surface area of chlorella sp. biochar produce from torrefaction is 2.66 m^2/g[44, 55]. The first step is pretreatment in which Algae biomass is washed, and then drying occurs. After this stage, the Algae sample is placed in the tube furnace for torrefaction. This process is done in the absence of oxygen by providing nitrogen as a media at 200 -300°C to produce biochar. Different Algae are used for the exclusion of heavy metals such as (arsenic, mercury, chromium, lead) and dyes.

2.3.4 Impact of thermochemical technique on biochar properties

Compared to lignocellulosic biomass, algal biochar has a lower yield. This could be because algal biochar has more minerals, which can also act as a catalyst during the pyrolysis process.[61]. This is confirmed by decrease in the biochar yield with increase in pyrolysis temperature and residence time. Ash content of Algae biochar is positively and negatively correlated with surface area and capacity of cation exchange respectively. Therefore, algae derived biochar has higher ash contents and so as the lower surface area. pH of biochar generally is the measure of oxygen functional group on the surface and pH of Algae biochar is reported to increase with increase in pyrolysis temperature from 250 ~ 600 ºC[62]. Due to enhancing pyrolysis temperature, the biochar's surface functionals changed from aliphatic to aromatic, with the development of aromatic rings and H deformation also being observed. [63].

2.4 Treatment of textile wastewater

Numerous methods are used for the treatment of textile wastewater treatment, which are reveal in Table 2: Treatment methods for textile wastewater .The main prospect of the present study is to treat through biosorption through Algae and its biochar.

Table 2: Treatment methods for textile wastewater [30]

Methods	Process technique
Physical	Ion exchange
	Membranes and membrane processes
	Adsorption using carbon nanotubes and zeolites
	Electrokinetic
	Coagulation
Chemical	Oxidative processes
	Ozonation
	Advanced oxidation by Fenton reagent
Photochemical methods	Photocatalytic degradation by irradiation
	Photochemical oxidation with H_2O_2

	Sodium hypochlorite	
Biological method	Aerobic	
	Anaerobic	

2.5 Biosorption through Algae

Algae are used for biosorption due to their high metal adsorption capacity, their cost-effectiveness, and their efficacy[64]. The removal of heavy metals from wastewater using Algae is good because they also have the ability to take other elements, such as potassium and phosphorus. For example, Chlorella preniodisa and Scenedesmus obliquus are used to remove heavy metals such as copper and zinc. The removal was greater than 70%, which is reported after 192 hr. of the experimental study[65]. The process of degradation of an organic pollutant by Algae is the same as that for the removal of heavy metal ions. The initial stage is rapid physiochemical (passive) adsorption. Biosorption was a beneficial exothermic and spontaneous process, as shown by the thermodynamic property of adsorption of phenol by Spirulina sp. LEB18[66].

The torrefied microalgal biochar (Chlorella sp.) adsorbed several dyes as tested on a laboratory scale in a working volume of 50 ml. The optimum condition to absorb these dyes is 150 rpm agitation rate at 30 °C temperature. The effects of the adsorbent dose were investigated at the various amount of biochar (0.1, 1, 2, and 5 g/L) and a starting dye concentration of 50 ppm[48].

Different Algae are utilized for the removal of dyes and heavy metals such as (arsenic, mercury, chromium, lead). Specific contaminants were tested in aqueous solution and then removed using microalgal-based biochar. The biochar's were synthesized and characterized. However, the majority of recent research is focused on evaluating the properties and performance of pristine microalgal biochar under regulated laboratory circumstances. Algae-based biochar can be tested for their actual efficacy by conducting tests on actual effluent samples containing a wide range of contaminants that imitate the conditions at the actual wastewater site[42].

The amount of adsorbent dosage is vital for the economic performance of batch adsorption. The percentage of removal of Congo Red dye is 2.16% at a dose of 0.1 g/L and increased by 98.0% at 3 g/L. After this point it remains constant. The percentage of Methylene blue removal enhanced from 11.82% to 94.60% with an increase in adsorbent dosage from 0.1 g/L to 5 g/L[67]. The extraction of Synazol Red dye, Remazol Black, Remazol Red, textile dye is removed from Algae. The results are shown in Table. 3.

Very limited work is reported on use of Algae biochar for removal of heavy metals and dyes from textile water. Moreover, utilization of lipid extracted biomass for biochar to remove heavy metals and organic molecules especially dyes is very limited[84].

Table 3: Biosorption capacity of dyes and heavy metals by Algae

Algae	Dye	Heavy Metal	Conc. Tested	Outcomes	Ref.
Raw biomass (Spirulina sp.)	-	Mercury (Hg) Cadmium (Cd)	Cadmium 3.816 mg/kg	Concentration of metal factor: 80 - 4250	[30]
				Capacity of Bioaccumulation	
				Cadmium (Cd) - 0.463 µg/kg biomass	
			Hg – 0.762 mg/ kg	Mercury (Hg) - 1.340 µg/kg biomass	

20

Raw biomass (Chlamydomonas *reinhardtii)*	-	Mercury, Cadmium, and Lead	100 mg/L	Freundlich biosorption isotherms is used to describe the equilibrium capacity of biosorption is	[68]
				Mercury Hg (II) - 0.0722 mg/kg	
				Cadmium Cd (II) - 0.0426 mg/kg	
				Lead Pb (II) - 0.0963 mg/kg;	
Raw Biomass (Ulothrix zonata)	-	Copper Cu (II)	5 - 52 mg/L	Langmuir adsorption model was fitted in adsorption isotherm	[69]
				Quick exclusion of copper (II) in the first 1200 s	
				Optimal pH for copper (II) elimination - 4.5	

Raw biomass (Spirogyra sp.)	Azo Dye	-	5, 12 and 17 mg/L	Removal efficiency of dye 35.3 - 64.0%	[70]
				Three repetitive runs show a similar biosorption rate.	
Raw biomass (Spirulina platensis)		Cadmium	40-200 mg/L	Removal efficacy 87.69% using Langmuir as a adsorption model	[71]
	-	Lead Pb (II)	25 - 210 mg/L	>90% removal	[72]
				Freundlich isotherm is best fitted for experiment	
Raw biomass (Chlorella sp.)	Methylene blue	-	100 mg/L	Removal efficiency is 83.04%	[73]
Raw biomass with CO_2 fixation (Scenedesmus obliquus)	-	Cadmium (Cd) (II)	2.6 - 7.7 mg/L & the flow rate is 18 mL/min	The adsorption capacity of 0.0384 g (breakthrough time of 930 min) had a flow rate of 6 ml/min and a	[74]

				Cd concentration of 0.0075 mg /L as an influent	

2.6 Biosorption through Algae biochar

Biochar have high adsorption capacity due to its carbonaceous property[75]. A mass-transfer process known as adsorption involves the accrual of dissolved solute pollutants on the surface of a solid phase to remove them from a liquid. The adsorbate is the substance that is adsorbed onto a solid surface, and the adsorbent is the substance that adsorbs the adsorbate. Soluble species are taken up by diffusion and adhere to the wide inner surface of the porous solid adsorbent during the adsorption method [76]. The adsorbent is in solid form in which heavy metals and dyes attach to the surface of Algae-derived biochar, having a large cluster with a pore size range of 10-100 μm. As compared to other feedstock (Sewage sludge, olive husk, pine saw dust) with Algae (Chlorella vulgaris, Chlamydomonas sp.)[77] because of its high yield, porosity, and adsorption capability, it is a viable feedstock for the manufacture of biochar. as reveal in Figure. 4.
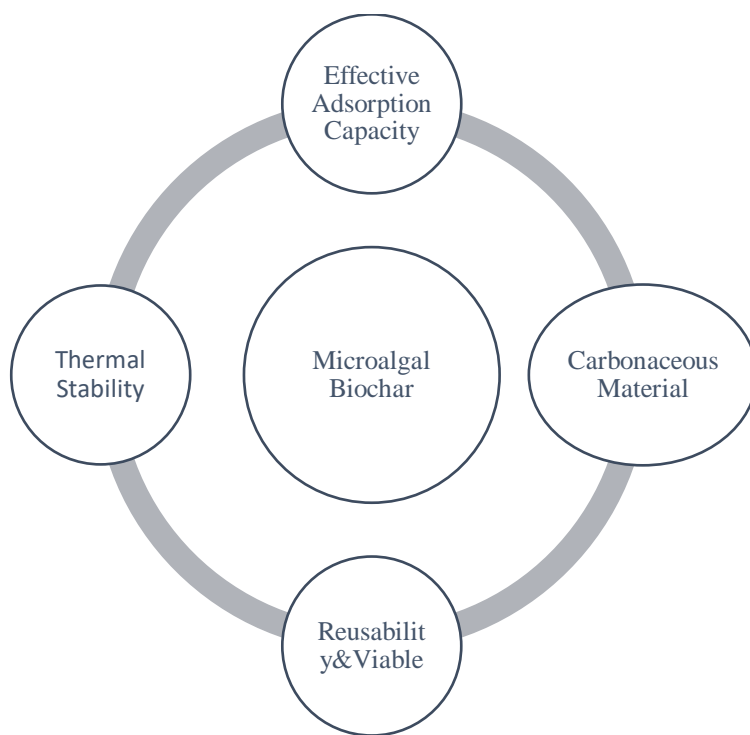
Figure 4: Properties of algal derived biochar[78]

2.7 Factors governing the biosorption of heavy metals and dyes

The biosorption ability of heavy metals and dyes in Algae-derived biochar is affected by its pH, surface charge, porosity, large surface area, richness of functional groups at the surface, and mineral components. Pollutants are eliminated thanks to the biochar's surface function group .as shown in **Figure 3.**
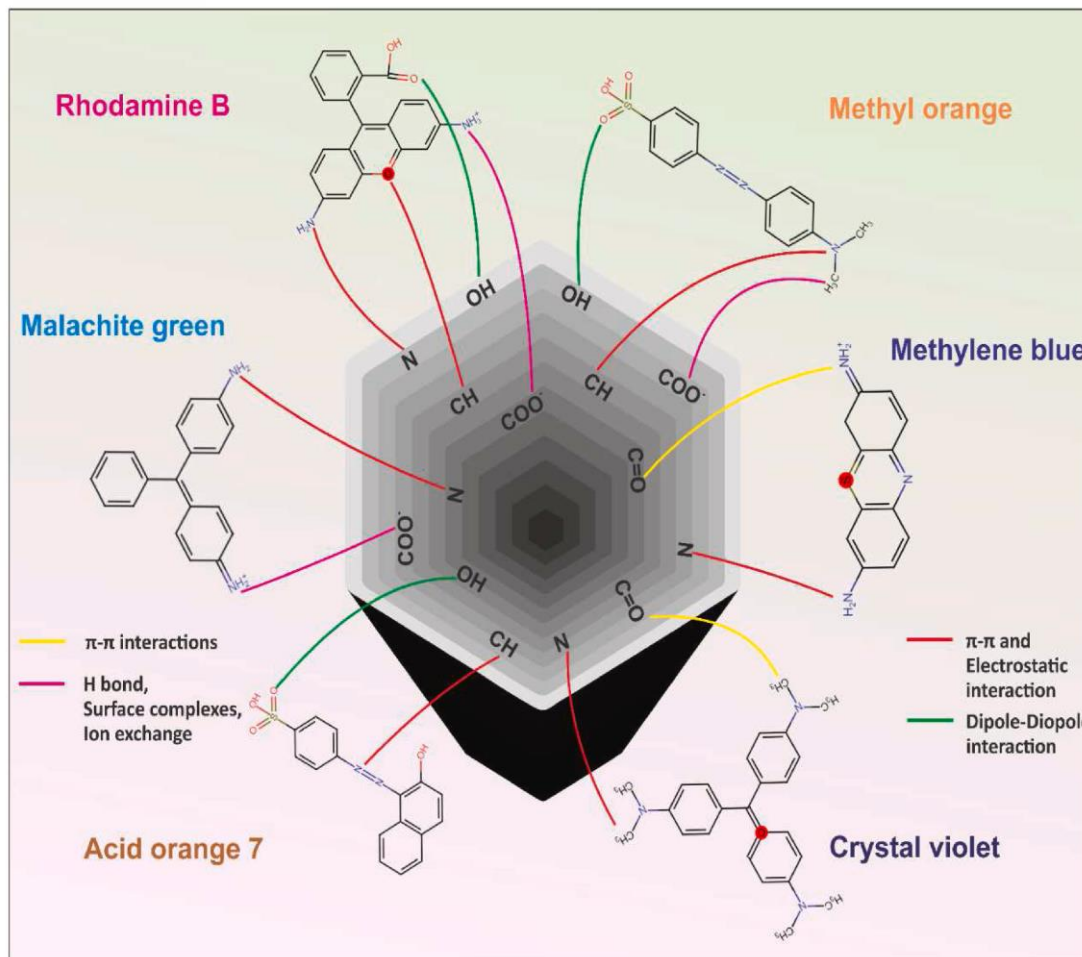
Figure 5: Role of surface functional groups on biochar and possible mechanism involved for dye removal from wastewater. *Reprinted with permission from Elsevier [79].*

The biochar's surface is acidic due to the presence of hydroxyl groups and basic due to the presence of carbonyl groups from the algae that produced the biochar. As a result, the treatment process will be optimized for the removal of both cationic and anionic compounds. By comparing the FTIR spectra of biochar before and after the adsorption process, one can see the effect of functional groups during the removal of organic molecules, as the intensity of peaks decreases, peaks move positions, and new peaks appear.[80].

2.7.1 pH

The pH plays a vital role in the surface charge of microalgal-based biochar. The pH of biochar is correlated to the presence of oxygen functionalities in the biochar and pH of Algae derived biochar are in the alkaline window (7.6 ~ 13.2) and it depends on pyrolysis temperature are well[81].

 The electrostatic attraction of carbonaceous material to impurities such as heavy metal ions is greatly influenced by pH_{pzc}. Because of its negative charge, biochar is capable of binding metal ions to solutions when the pH exceeds pH_{pzc}. When the solution pH is less than that of biochar pH, its positive charge emphasizes binding to metal anions at higher pyrolytic temperatures, the negative functional groups (e.g., carboxylic acid, aldehyde, alcohol) on biochar would be lowered, resulting in a biochar surface with a lower negative charge[82, 83]. The solution pH plays an important role to facilitate the interactions of surface functional groups on the adsorbent and the ionic state of dye for its removal. In an acidic medium, H^+ ions increased in the system, resulting a more positive charge on the surface of the adsorbent due to higher concentration of H^+ and subsequent higher interaction for a negative dye molecule[84].

2.7.2 Physical characteristics

The microspores, pore volume, bulk density, and surface area are all examples of physical properties. In terms of volume, the bulk density of algae-based biochar was 780 g/L. Biochar made from algae has a smaller surface area than biochar made from lignocellulosic biomass. [77]. However, as pyrolytic temperatures rise, the surface area of carbonaceous material increases. For example surface area of biochar derived from spirulina residues enhanced from 0.015 to 0.025 m^2/mg as the pyrolytic temperature increased[85]. Except for the Chlorella sp. biochar recovered by sonication, all other biochar's showed a relatively high specific surface area (0.266 m^2/mg) and a pore volume of 0.00061 cm^3/mg[55]. Furthermore, the biochar surface area made from Scenedesmus dimorphous and Spirulina platensis was quite large. The enormous surface area and pore volume of biochar make it an excellent adsorbent of contaminants, and its ability to retain metal ions on the surface and within the pores makes it an excellent absorbent. Different

Algae also produce charcoal; for example, Chlorella biochar is a mixture of short rods and fine powder, Chlamydomonas biochar is a porous sheet, and Colostrum biochar is a crushed particle[86]. Moreover, ash content of biochar derived from Algae biomass are higher than other biomass possibly due to high contents of minerals[77].Growth environment of Algae species play a role in the minerals content of ash. Algae grown in sea water will have higher content of Na and K than the one in fresh water. Presence of these salts can lead to different surface structure properties as well. Presence of Ca^{+2} in Algae biochar enhanced the uptake of four different dyes at various pH though modulation in zeta potential. Therefore, presence of these heteroatoms makes the biochar derived from Algae an attractive option for energy and sensing and environmental application due to increase in cation exchange capacity. Presence of Ca^{+2} and Na^+ ions are reported to play a significant role in the removal of dyes due to shirt in zeta potential[87].Carbon to nitrogen (C/N) ratio is low is Algae dried biochar than its counterpart from lignocellulosic biomass[77]. But presence of high ash content in Algae biochar need further post treatment which is not desired for lignocellulosic biomass. The Algae derived biochar are generally less porous than their lignocellulosic counterpart and have sheet like structure.

2.7.3 Surface functional groups

The functional groups (-O.H., -COOH, etc.) on the surface of biochar play a vital role in determining the water-hating or water-loving nature of biochar. The adsorption of metallic ions is accomplished by electrostatic attraction, complexation, and surface precipitation, all of which are capable of interacting with heavy metals. However, important functional groups such as -O.H. and -C.H. are reduced due to enhancing the pyrolytic temperature. The result of this -led to the production of less biochar as well as low acidic functional groups (such as carboxyl and hydroxyl groups) when the pyrolytic temperature was raised; however, the yield of basic functional groups (such as $-NH_3$ groups) increased along with pH, ash content, and carbon stability, as well as gaseous yield. A high pyrolytic temperature results in the enhancement of surface area and micropore volume of carbonaceous material and decreases the water-loving properties, making it more effective at solubilizing organic pollutants but diminishing its adsorptive capacity for inorganic pollutants (e.g., heavy metals). In addition, its high hydrophobicity makes it resistant to

wetness. Biochar enhanced the adsorption capacity of heavy metals due to its hydrophilicity property as well as the presence of oxygen as a functional group. Adsorption is also enhanced by the existence of basic or acidic functional groups in biochar, such as phenolic, lactonic, and carboxylic groups, which interact with the chemical interactions produced between the adsorbent and the pollutants[47, 86, 88, 89].

When biomass is burned, it changes into biochar, which has different or less functional groups than the original biomass. The functional group of biochar made from their ashes can be affected by the type of biomass and even the algae it comes from [c]. The fact that algal biomass has functional groups on its surface also makes it different from lignocellulosic biomass, which is made of different things. During pyrolysis, there were a number of thermochemical changes that affected the functional groups of the biomass. These changes led to biochar with a wide range of properties. Figure 6 shows the FTIR spectra of Chlorella vulgaris (CHLO), Spirulina sp. (SPI), Nannochloropsis sp. (NAN), nutshell lignocellulosic biomass (a), and biochar. (NUT). C-N, N-H, and C-O-C bands can be seen in both algae biomass and biochar, but they can't be seen in nutshell biomass because amides are found in protein and ethers and block these bands from showing up. [77].

Biochar's acidity reduced and its basicity increased as pyrolysis temperature rose. Biomass from fast pyrolysis is dominated by hydroxyl and carboxyl function groups, while biomass from delayed pyrolysis contains aromatic C-H bonds [ref b]. And during pyrolysis of Algae biomass, alkali and alkali earth metals are present encourages the synthesis of O-containing functional groups in biochar.[62].
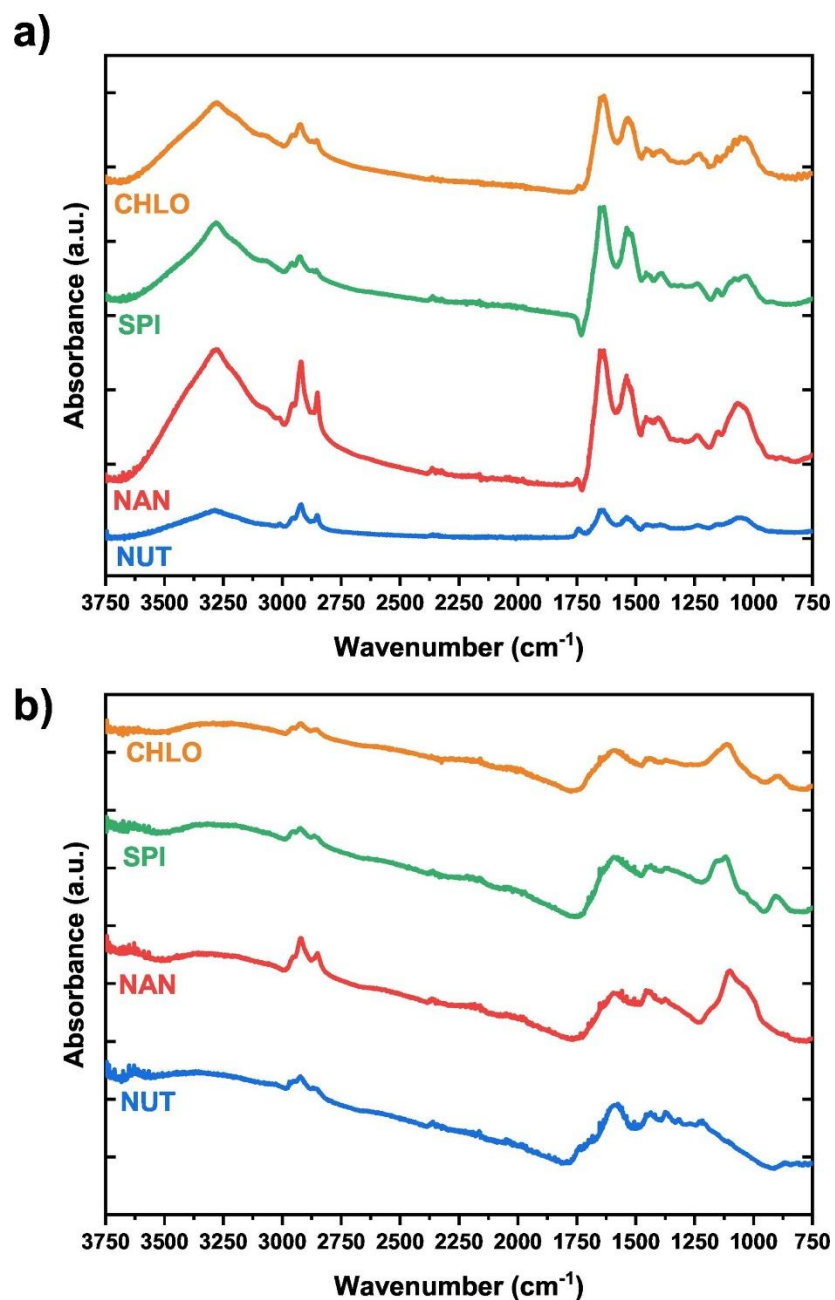
Figure 6: Variation in functional groups in the raw feedstocks (a) an in the biochar (b).Reprinted by permission from Elsevier[77].

These variations showed that Algae derived biochar will function differently that lignocellulosic biomass or municipal biowaste. The main difference between the Algae derived biomass and lignocellulosic biomass is the presence of C-O band in the latter which is beneficial for its application for heavy metals removal and catalytic process.

Figure. 7. showed the various mechanism involved for removal of inorganic and organic molecules through biochar physical and chemical characteristics.
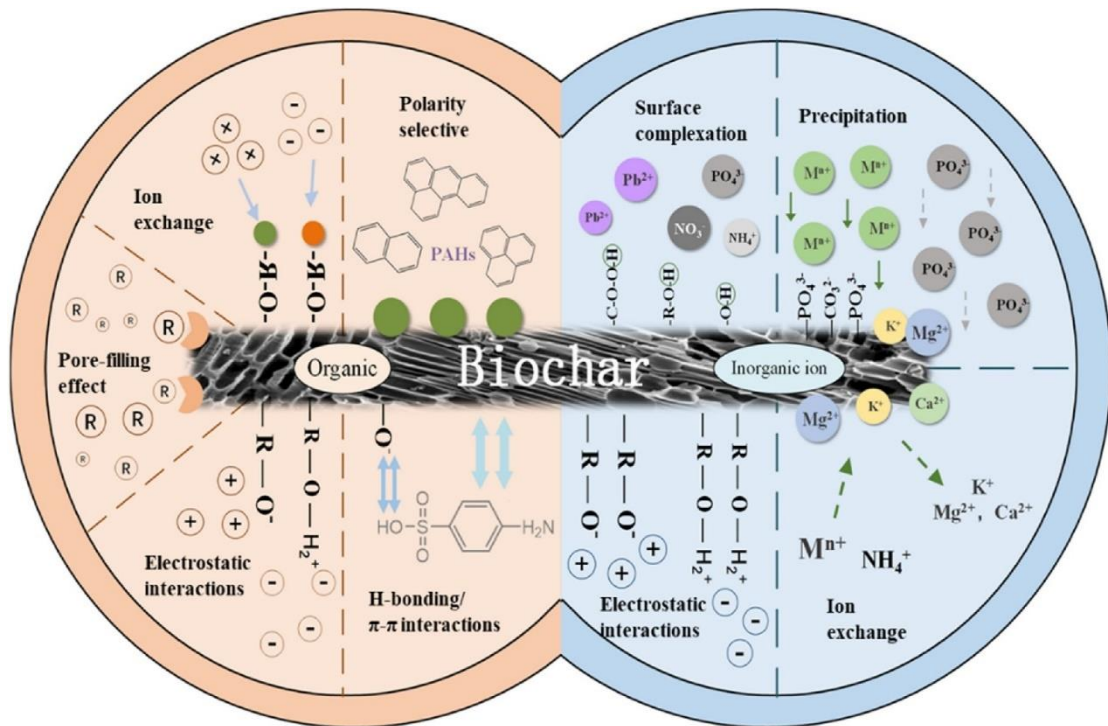
Figure 7: Possible mechanisms of organic and inorganic pollutants removal using biochar. Reprinted by permission from Elsevier[90].

2.8 Comparison of Algae-based biochar and other carbonaceous material:

The structure of Algae derived biochar differs from that of lignocellulosic biomass-produced biochar through pyrolysis process[91]. Biochar are synthesis from different biomass such as Bamboo cane, Waste poplar leaves, Waste Mangosteen shell, rice straw, risk husk etc. The production of biochar from Algae through slow pyrolysis is 56.3-66.2% at temperature range of 300-700 ˚C. Other biomass source such as sewage sludge produce biochar 39-52% at temperature range of 350-950 ˚C. Olive husk produce biochar 9.4-44.5 wt% of biochar yield at temperature range of 400-1000 ˚C[57].

Chapter 3

Materials and Methods

3.1 Material

The algae culture as feedstock was collected from the Ravel dam in Islamabad, Pakistan. Chemical reagent Potassium dichromate ($K_2Cr_2O_7$, molecular weight 294.18, CAS number 7779-50-9, 99 % purity), 1,5 diphenyl carbazide ($C_6H_5NHNHCONHNHC_6H_5$, molecular weight 242.28, CAS number 140-22-7, 97 %), Congo Red Dye, (Phosphoric acid (H_3PO_4, molecular weight, 98.00, CAS number 7664-38-2), methyl alcohol (CH_3OH, molecular weight 32.04, CAS number 67-56-1, assays 99.7 %) hydrochloric acid (HCl, molecular weight 36.46, CAS number 7647-01-0, assays 36.5-38 %), was procured from Sigma Aldrich. Deionized and ultra-pure distilled water was purchased from Reliance Enterprises. Block-A Soan Garden, Islamabad.

3.2 Biochar Preparation

The method used for the preparation of biochar is slow pyrolysis. Prepare a sample of algal biomass before starting the pyrolysis process. First, the collected algal biomass is washed with ultrapure distilled water to remove impurities. The clean algae were sun-dried for 2 days followed by drying in an oven for 24 h at 105 ℃. The algae was ground using a laboratory-scale grinder to convert it into a 0.23 mm particle size of 0.23 mm to make the sample pulverized. The dried pulverized algae were used for the synthesis of biochar through slow pyrolysis. Briefly, 10 g of the sample were placed in an electrical tubular furnace (maximum limit 1200 ℃) and pyrolyzed at a temperature of 500 ℃ at a heating rate of 10 ℃/min and 60 min of residence time. The process occurs in starved oxygen using nitrogen (N_2) as an inert environment. Three products (biochar, liquid, and gas) are formed during slow pyrolysis, but the main product is biochar. After slow pyrolysis, the biochar was allowed to cool in the furnace. The graphic planning for the synthesis of algae-derived biochar is shown in Figure.8.
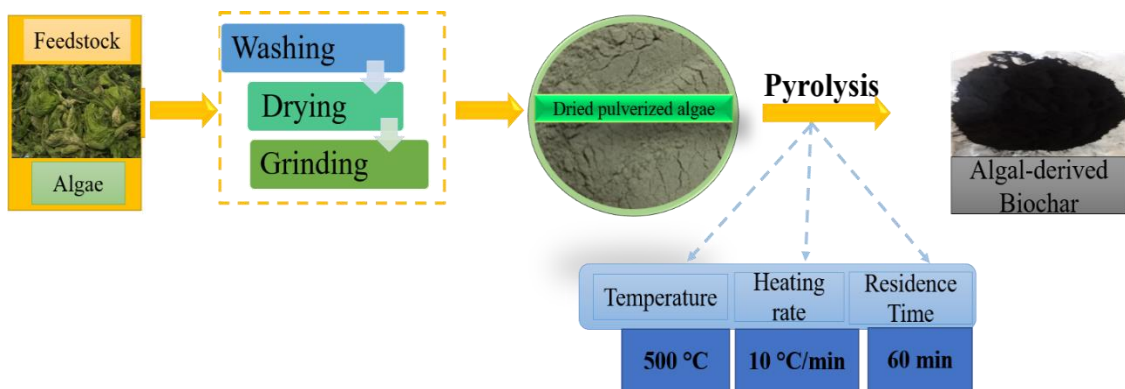
Figure 8:Synthesis of algal-derived biochar through slow pyrolysis

3.3 Preparation of Cr (VI) and Congo Red solution

The stock solution (1000 ppm) of Cr (VI) was prepared using 0.283 g of potassium dichromate ($K_2Cr_2O_7$). First, dry in the oven at 100 °C for 60 min and then add it with 100 ml of deionized water in a volumetric flask [92]. The absorbance of the stock solution was measured using a UV-vis spectrophotometer (SP-UV 300, PerkinElmer company) at 540 nm, using a reagent DPC. The DPC solution is obtained by adding DPC to 250 ml of methanol [25]. The absorbance of the solution calibration curves was plotted and analyzed by the coefficient of determination (R^2).

The stock solution of 1000ppm Chromium prepare add 1g of Congo red Dye powder in 1L distilled water. Further, working solution are prepare by diluting the stock solution or apply the formula $M_1V_1 = M_2V_2$. The accuracy of stock solution is check by UV-vis spectrophotometer at 500 nm.

3.4 Batch adsorption experimental data

To evaluate the removal efficacy, adsorption isotherm and kinetic model by non-linear analysis, adsorption data were obtained for modeling by series of batch experiments, which were conducted by taking 50 ml of Cr (VI) solution and 50 ml of Congo Red Dye solution in 100 ml Erlenmeyer flask as depicted in Table 4. The required quantity (0.1 g) of algae biochar was added to the solution with pH 2 and the flask was placed on a mechanical shaker at an agitation speed of 150 rpm. The experiment was carried out by changing the concentration (1, 10, 25, 50, 100, 125, 150, 200 ppm) at different intervals

of time (2.5, 5, 10, 15, 30, 60, 120, 240 min) to investigate Cr (VI) and Congo Red Dye adsorption on algal derived biochar and measured the final Cr (VI) concentration using a UV-Vis spectrometer at 540 nm. The removal efficacy (%) and adsorption capacity (mg/g) were obtained by Eq. 1, Eq. 2 and Eq. 3 [93].

$$Chromium\ Removal(\%) = \frac{C_O - C_t}{C_0} \times 100 \tag{1}$$

$$q_t = \frac{C_o - C_t}{M} \times V \tag{2}$$

$$q_e = \frac{C_o - C_e}{M} \times V \tag{3}$$

where C_o represents the initial concentration, and C_e and C_f are the equilibrium and final concentrations of Cr (VI). M (mg) is the mass of the algae biochar, and V (ml) is the volume of the chromium solution.

Table 4: Adsorption data of algal biochar for the removal of chromium and Congo Red Dye with various concentration (1-200 mg/L) at different interval of time (2.5-240 min)

Time t min	Initial concentration C_o (mg/L)	Adsorption capacity (CrV1) q_t, q_e (mg/g)	Adsorption capacity Congo Red Dye q_t, q_e (mg/g)
2.5	1	0.19	0.13
2.5	10	2.08	1.59
2.5	25	5.60	4.25
2.5	50	11.41	9.28
2.5	100	22.98	19.68
2.5	125	29.64	25.18
2.5	150	36.49	31.32
2.5	200	49.77	43.44
5	1	0.31	0.27

5	10	3.31	2.83
5	25	8.73	7.41
5	50	17.89	15.32
5	100	36.06	31.66
5	125	45.81	40.15
5	150	55.96	50.48
5	200	76.42	69.20
10	1	0.38	0.35
10	10	3.94	3.57
10	25	9.88	9.13
10	50	19.90	18.50
10	100	40.20	37.56
10	125	50.35	47.71
10	150	60.85	57.95
10	200	82.16	79.17
15	1	0.44	0.43
15	10	4.56	4.36
15	25	11.63	11.16
15	50	23.30	22.52
15	100	46.87	46.14
15	125	58.90	57.94
15	150	69.01	67.89
15	200	91.56	89.40
30	1	0.46	0.45
30	10	4.64	4.63
30	25	11.81	11.62
30	50	23.69	23.47
30	100	47.59	47.00
30	125	59.74	58.97

30	150	70.15	68.39
30	200	92.98	90.85
60	1	0.48	0.48
60	10	4.88	4.80
60	25	12.06	11.88
60	50	24.11	23.67
60	100	48.20	47.17
60	125	60.01	58.98
60	150	71.66	69.40
60	200	94.19	91.87
120	1	0.489	0.480
120	10	4.88	4.80
120	25	12.10	11.90
120	50	24.14	23.68
120	100	48.26	47.22
120	125	60.06	59.00
120	150	71.77	69.4
120	200	94.65	91.88
240	1	0.48	0.48
240	10	4.88	4.80
240	25	12.10	11.90
240	50	24.15	23.68
240	100	48.29	47.25
240	125	60.12	58.88
240	150	71.80	69.48
240	200	94.68	91.90

3.5 Non-linear adsorption isotherm model

The adsorption isotherm is established [94] when the chromium-containing phase comes into contact with algal-derived biochar for a sufficient time. The adsorption isotherm is used to describe the adsorption mechanism. There are numerous non-linear adsorption isotherms that can be used to describe how adsorption works.

3.5.1 Langmuir isotherm

The Langmuir isotherm is a monolayer adsorption model that assumes that adsorption may occur only at precisely localized sites. The non-linear expression can be demonstrated as Eq. 4 [95].

$$q_e = \frac{Q_0 b C_e}{1 + b C_e} \tag{4}$$

q_e is adsorbed at equilibrium (mg/g), C_e is the solute at equilibrium (mg/L), Q_0 (mg/g) are constants associated with the adsorption capacity and b (l/mg) is the constant energy of adsorption.

3.5.2 Freundlich isotherm

The Freundlich isotherm is applied to multilayer adsorption, which explains the relationship between nonideal and reversible sorption, and it is done on a heterogeneous surface. The Eq. 5 [96] is expressed as follows

$$q_e = K_F C_e^{1/n_F} \tag{5}$$

K_F [mg/g (l/mg)$^{1/n_F}$] denotes the adsorption capacity and Freundlich constant represented by "n_F".

3.5.3 Dubinin-Radushkevich (D-R) isotherm

D-R is an empirical isotherm model that is used to describe homogeneous and heterogeneous surfaces for the adsorption process followed by the pore filling mechanism [97]. It is formulated for the pore-filling mechanism in the adsorption process. The non-linear form of the D-R isotherm model can be demonstrated as Eq. 6 and Eq. 7 [98].

$$q_e = q_s \exp(-K_{DR}\varepsilon^2) \tag{6}$$

$$\varepsilon = RT \ln\left(1 + \frac{1}{C_e}\right) \tag{7}$$

where q_s is constant related to the adsorption capacity(mg/g), K_{DR} represented as the mean free energy of adsorption (mol^2/kJ^2), R (J/mol K) is the general gas constant.

3.5.4 Temkin model

The interaction between the heterogeneous surface of adsorbate molecules and adsorbent molecules is illustrated by a Temkin isotherm model, which features a uniform distribution of maximal binding energy. The non-linear form is demonstrated in Eq. 8 [99].

$$q_e = \frac{RT}{b_T} \ln A_T C_e \tag{8}$$

where, b_t (kJ/mol) is the Temkin isotherm constant, and A_T represents the equilibrium binding constant of the Temkin isotherm (L/g).

3.6 Adsorption kinetics

The kinetics of adsorption provides information about the pathway and mechanism involved in adsorption. It also determines the time required to reach equilibrium, by controlling the adsorption rate [100]. Studies [99, 101] have indicated that the adsorption model using the linearization technique is not a reliable technique for predicting adsorption kinetics. Therefore, the non-linear method will be a good way to predict the kinetics of adsorption. To analyze the kinetic parameters of adsorption processes, various non-linear kinetic forms are used.

3.6.1 Non-linear PFO kinetic model

According to PFO, the difference between the equilibrium concentration and the amount of the solute adsorbed with time is directly proportional to the rate of change in the solute sorption with time. The non-linear form is expressed in Eq. 9 [102].

$$q = q_e[1 - \exp(-k_1 t)] \tag{9}$$

Here, q_e (mg/g) is the equilibrium adsorption removal capacity (mg/g), q_t is the variable time adsorption capacity (t), and k_1 is the constant PFO rate.

3.6.2 Non-linear PSO kinetic model

The PSO predicts the behavior over the entire domain of adsorption on the premise that the rate-limiting phase is chemisorption and the adsorption rate depends on the adsorption capacity and not the adsorbate concentration. The non- linear form is depicted in Eq 10 [102].

$$q = \frac{k_2 q_e^2 t}{1 + k_2 q_e t} \tag{10}$$

k_2 is the rate constant of the PSO

3.6.3 Non-linear PNO Kinetic Model

The PNO adsorption kinetic model is an empirical rate equation that is known to determine the kinetic analysis, but is not evaluated with the PFO and PSO kinetic parameters. [103]. The Eq. 11 [99] express the adsorption rate of the non-linear form of PNO.

$$q = q_e - [q_e^{1-n} + (n-1)k_n t]^{\frac{1}{n-1}} \tag{11}$$

where n represents the nth order and k_n is the rate constant of PNO.

3.6.4 Intraparticle diffusion

Intraparticle diffusion is another kinetic model that was used to describe the sorption mechanism for both pore and film diffusion by Weber and Morris. The formula was presented in Eq. 12 [104].

$$q = k_i t^{\frac{1}{2}} + C_i \tag{12}$$

where, k_i is the diffusion constant of the intraparticle diffusion (mg/g min$^{1/2}$) and C_i is the intercept or surface adsorption.

Using the Solver add-in for Microsoft Excel, all model parameters were tested for the non-linear regression technique. To determine the fit model, using the SSE and the

determination coefficient (R^2) for each parameter, which was used to identify the best fit model for the experimental data, as shown in Eq. 13 [97].

$$R^2 = \frac{\Sigma(q_{e,th} - \bar{q}_e)^2}{\Sigma(q_{e,th} - \bar{q}_e)^2 + \Sigma(q_{e,th} - q_{exp})^2}$$
(13)

3.7 Artificial Neural Network (ANN)

ANN models are used to develop the network architecture to achieve the chromium and Congo Red Dye removal efficiency target model using the TIBCO Statistica 13.5 software (StatSoft, USA). The network type is multilayer perceptron which is utilized for non-linear progression, basically composed of input, hidden, and output neurons, which is shown in Figure 9. In the present study, to develop the model of target values, two input layers (time and concentration) are used as an input neuron, and the output layer is removal efficacy. The data set is specified into three categories, training (70 %), testing (15 %), and validation (15 %) [105].

The activation function of the input layer is the identity function, while MLP activation functions of hidden and output neurons are identify, logistic, Tanh, exponential and Sine. The neural network is somehow trained through supervised learning by reducing the sum of squared error. Types of prediction are standalones and ensembles, which include inputs, targets, input, and residuals. The code generator in this study is PMML 4.2. ANS is the characteristic of the SANN regression strategy, which compares different networks and chooses the best model based on comparisons that neglect dilated time [38].
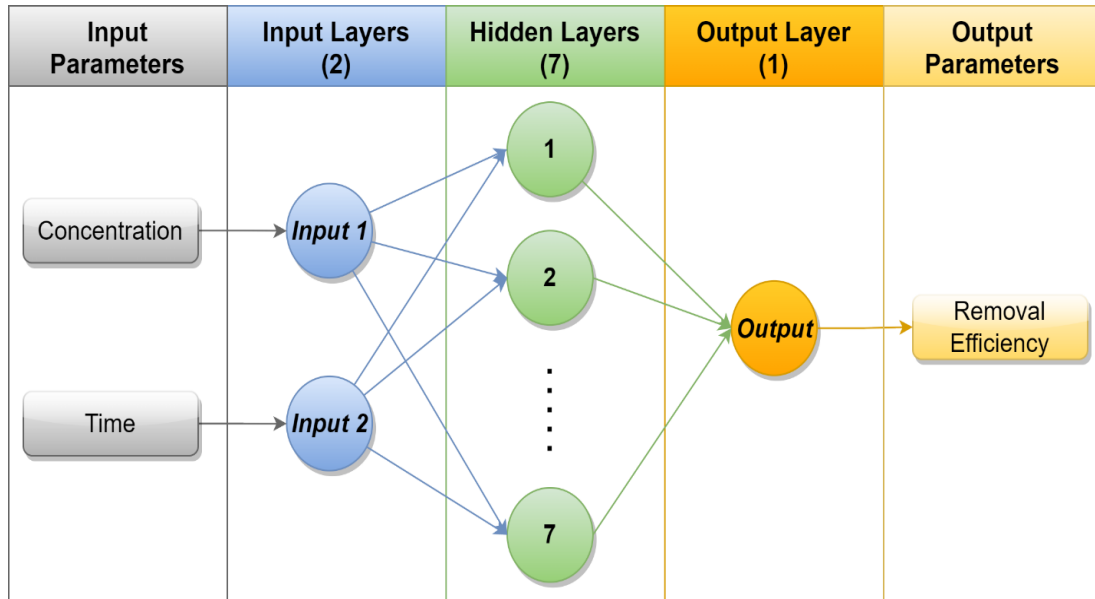
Figure 9: Network topology of ANN

3.8 Characterization

The characteristics of algae biomass and biochar before and after adsorption are estimated using the characterization techniques SEM, EDX, and FTIR. The surface morphology and pore size of the algal biomass and its derived biochar are analyzed by scanning electron microscope (SEM). The mapping of biochar surface morphology after adsorption to chromium and Congo red identification is analyzed by EDX, which is coupled with SEM (JEOL JSM-6490A). Identification of the functional group of algal biomasses, algal-derived biochar, and after adsorption of Cr (VI) is analyzed by a FTIR spectrophotometer (Perkin Elmer Spectrum 100) in a range of 400-4000 cm^{-1}.

Chapter 4

Result and Discussion

Biochar was prepared by heating algae sample at 500 °C for 60 min with a heating rate of 10 °C/min. The yield of biochar obtained under these conditions was 81.87%.

4.1 Effect of concentration and time for removal efficacy and adsorption capacity

4.1.1 Removal efficacy

Figure 3 and Figure 4 shows the efficacy of chromium removal and Congo Red Dye by algal biochar. The result demonstrates that the removal efficacy of chromium and Congo red dye increases with respect to time and, at 60 min, the process almost reached equilibrium. After the equilibrium time, there is no significant removal of chromium by changing the adsorption time. Therefore, 240 min was the time selected for chromium and Congo Red Dye adsorption on the surface of algal derived biochar to achieve maximum removal efficacy [40]. The reason is that initially the concentration difference between the adsorbate and the adsorbent is high, which overcomes resistance to mass transfer of chromium ion between the solid and aqueous phases. The effect of metal ion concentration shows that to increase the metal ion concentration from 1 to 200 mg/L the removal efficacy increases, but after 10 min the removal efficacy of high metal ion concentration (125, 150 and 200 mg/L) are low compared to other Cr (VI) concentrations and at 60 min the trend changes, the low concentration of metal ion shows high removal efficacy. This pattern may be caused by the fact that the concentration difference between Cr (VI) in the solution and the adsorbent increases with increasing initial concentration of Cr (VI). This difference may have enhanced the force and rate of mass transfer between the liquid and solid phases [106], promoted the migration of Cr (VI) to the surface of algae biochar, thus further improving the adsorption reaction, and initially more vacant sites are available to adsorb Cr (VI) and Congo red Dye [107] on the surface of algae biochar, but there will be a time when there are no more vacant spaces present and those metals that already adsorb

on the surface of algae biochar repel the incoming metal ion and decrease the efficacy of a high concentration compared to the low concentration of Cr (VI). Now, the result shows that the removal efficacy of chromium (1 mg/L, 10 mg/L, 25 mg/L, 50 mg/L and 100 mg/L, 125 mg/L, 150 mg/L and 200 mg/L) are 97.88, 97.743, 96.84, 96.602, 96.59, 95.74 and 94.68 %, which evaluates that the maximum removal efficacy (97.843%) increases at 1 mg/L Cr (VI) shown in Figure 10 (a) and (b). The removal efficacy of Congo Red Dye (1-200 mg/L) are 96.1404286, 96.0739143, 95.25248, 94.7532257, 94.5082057, 94.2133646, 92.6408038, 91.9006029 are shown in Fig 11 (a) and (b).The result is in agreement with previous work[108, 109].
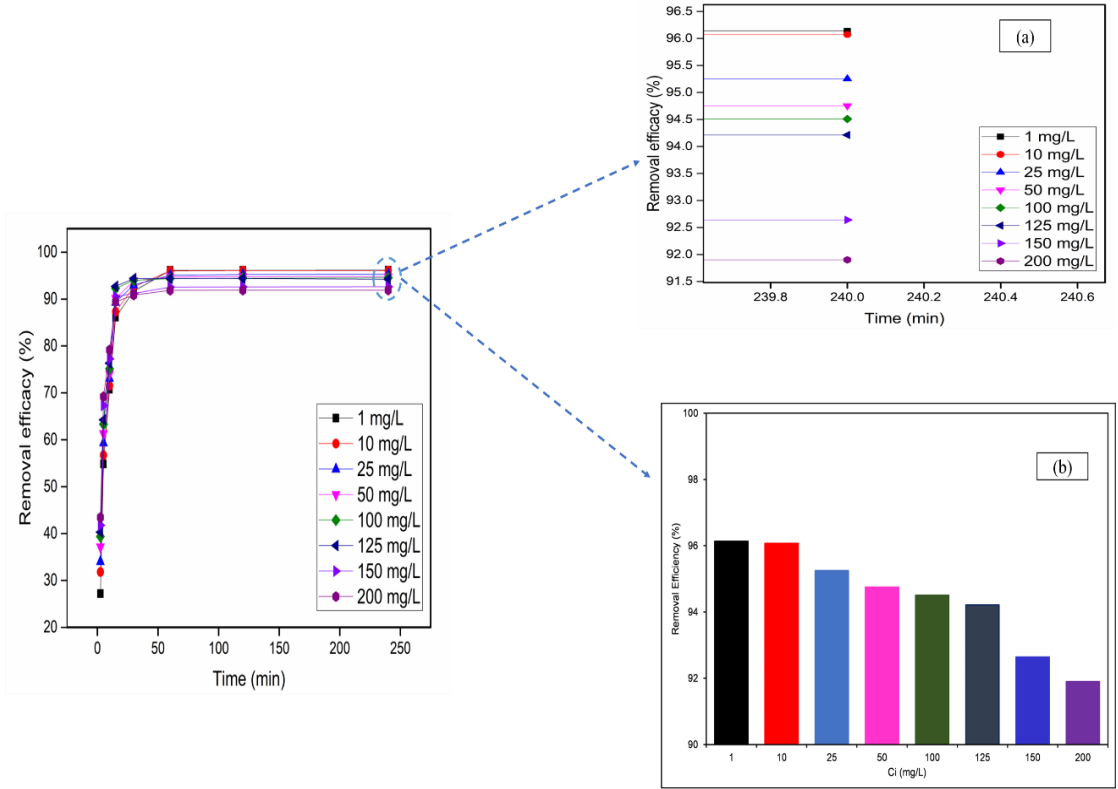
Figure 10: Removal efficacy of Cr (VI) with different time and concentration (a) Removal efficacy at 240 min (b) Removal efficacy with different concentration of chromium
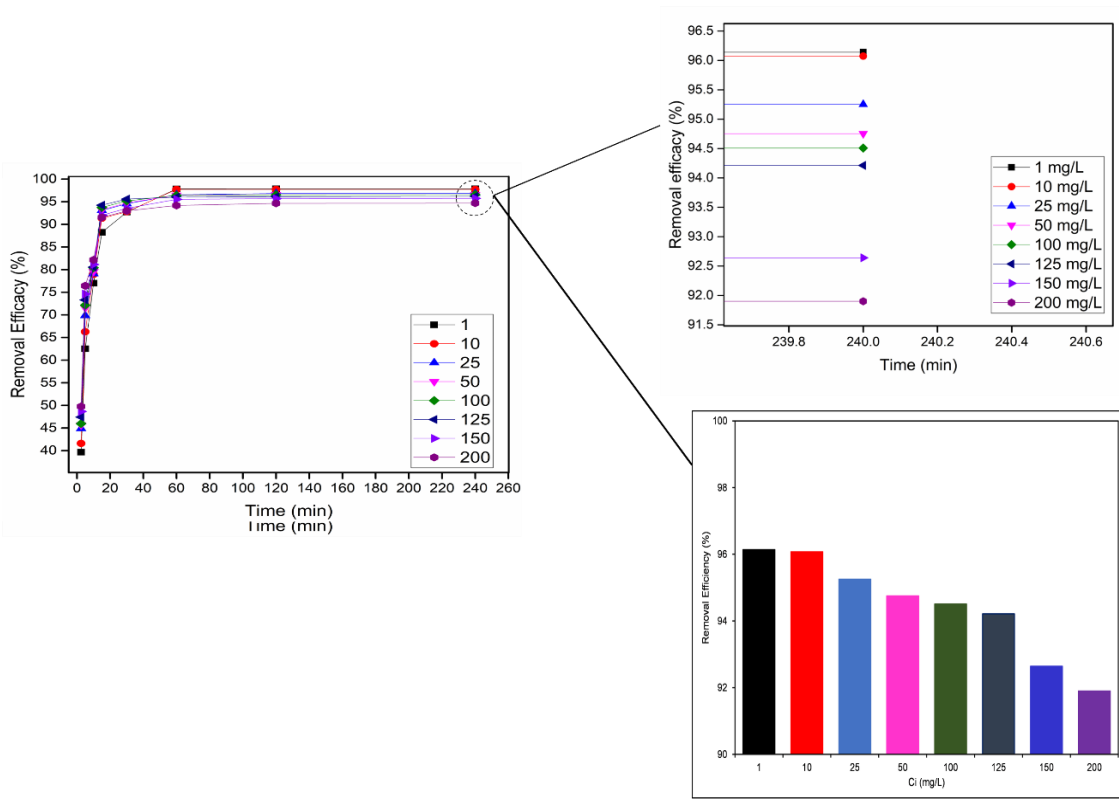
Figure 11: Removal efficacy of Congo red dye) with different time and concentration (a) Removal efficacy at 240 min (b) Removal efficacy with different concentration of Congo red dye

4.1.2 Adsorption capacity

Figure 12 and Figure 13 shows the adsorption capacity of algal biochar to adsorb chromium and congo red dye. The results show that the capacity to uptake Cr (VI) and congo red dye increases as the time and initial concentration of Cr (VI) and CRD ions increase. The trend shows that initially the adsorption capacity of the whole metal ion concentration increases because of the enhancement of the concentration difference between the chromium solution and algal biochar and the presence of large numbers of vacant sites available on the surface of the adsorbent, but time comes when it reaches equilibrium and little adsorption of Cr (VI) and congo red dye occurs on the surface of the algal biochar due to the unviability of the vacant surface or the repellent of the incoming metal ion. The adsorption capacity of the result shows that the Chromium (1mg/L,

10mg/L, 25mg/L, 50mg/L and 100 mg/L, 125 mg/L, 150 mg/L and 200 mg/L) are 0.489, 4.88743, 12.106, 24.151, 48.295, 60.124, 71.808, 94.687 mg/g at 240 min express in Figure 12 (a). The adsorption capacity of Congo Red Dye for (1-200 mg/L) are 0.4807, 4.8037, 11.9066, 23.6883, 47.2541, 58.8834, 69.4806, 91.9006 mg/g. The trend of adsorption capacity was previously recorded [106].
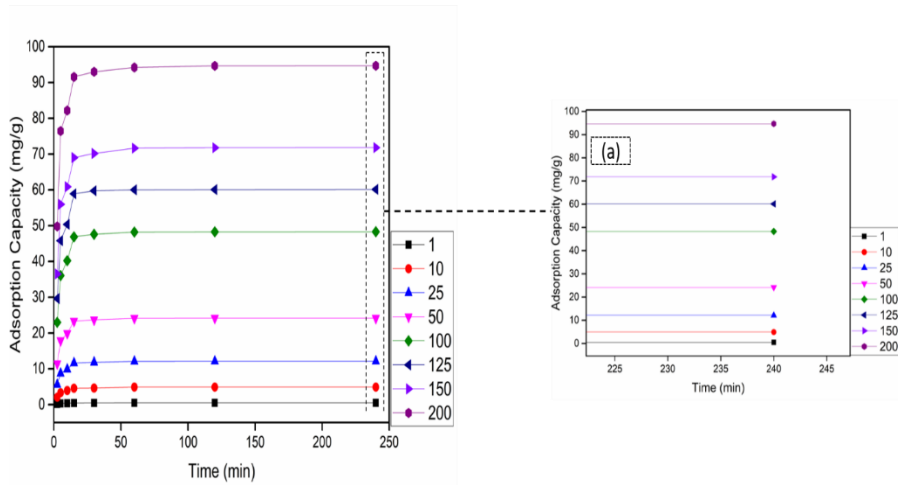
Figure 12: Adsorption capacity of algal-derived biochar for Cr (VI) removal (a) adsorption capacity of (1-200 mg/L) concentration of Cr (VI) concentration at 240 min.
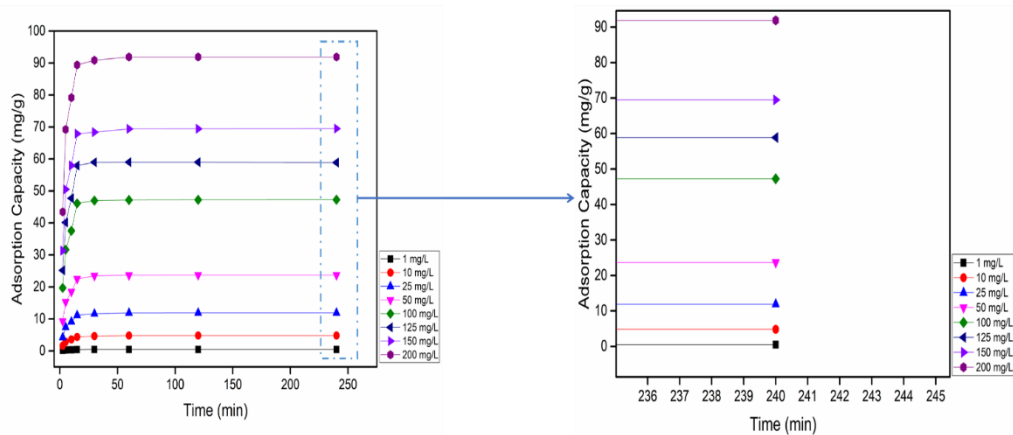
Figure 13: Adsorption capacity of algal-derived biochar for Congo red dye removal (a) adsorption capacity of (1-200 mg/L) concentration of Congo red dye concentration at 240 min.

4.2 Analysis of non-linear fitting of isotherm model

Figure 14 depict Langmuir, Freundlich, Dubinin-Radushkevich, and Temkin adsorption isotherms of the chromium on algal-derived biochar by non-linear analysis. The values of the isotherm parameters, their standard errors, and the correlation coefficients for each parameter are shown in Table 5. The present study shows that the Langmuir saturation capacity (Qe) is 186.937 mg/g and the value of the binding affinity of the active site to Chromium species or the Langmuir constant (b) is 0.098 ml / mg. The most important parameter of Langmuir model is separating factor $(R_L \frac{1}{1+bC_0})$ which give information about the favorability of adsorption process. The process is irreversible (R_L=0), linear (R_L=1), favorable(0<R_L<1) and unfavorable (R_L>1)[110, 111]. The R_L value obtained was 0.112 which shows that the adsorption process is favorable in the present study. The correlation factor is 0.999 and the sum of the square analysis is 11.883.

In the Freundlich model, the obtained value of the adsorption capacity (K_F) is 19.312 (mg/g) and the Freundlich constant (n_F) is 1.452. The value of $1/n_F$ is used to determine the favorability and surface heterogeneity [111, 112]. The value of 1/nF is 0.688 which shows that the current adsorption process is favorable, lying in the range (0-1) [113]. The R^2 and SSE values in this model are 0.991 and 81.018, respectively.

The acquired values of the D-R model parameters are shown in Table 5. The table shows that the adsorption capacity q_s is 69.766 mg/g, the activity coefficient K_{ad} is 8.457E-07, the R^2 value is (0.938) and the SEE value is 991. 567. The other model is the Temkin model, the acquired value of the binding energy constant 12.006, the Temkin isotherm constant (170.950), the correlation factor (0.757 and SSE (2012.709) for Cr (VI).

The same model studied for the removal of congo red dye shown in Fig15. The result shows that Langmuir model is best model for describing the adsorption mechanisms, having 0.996 R^2 value and 30.823 sum of square error. The present study shows that the Langmuir saturation capacity (Qe) is 179.95244 mg/g and the value of the binding affinity of the active site to Congo red dye (b) is 0.0625 ml / mg. The separating factor is

45

0.16219356 which show that adsorption model is favorable. The parameters of other model explained in Table 6.

Comparing the R^2 and the SSE values to predict the best fitting model in the present study. The results show that the D-R and Temkin models are not as compared to another model and also indicate that the Langmuir model is more acceptable for the adsorption isotherm. So, the adsorption characteristic of the experimental system may be the result of monolayer adsorption.

Therefore, by comparison, the order of the isotherm that best fits the experimental data in this study is **Langmuir > Freundlich >Dubinin-Radushkevich > Temkin**
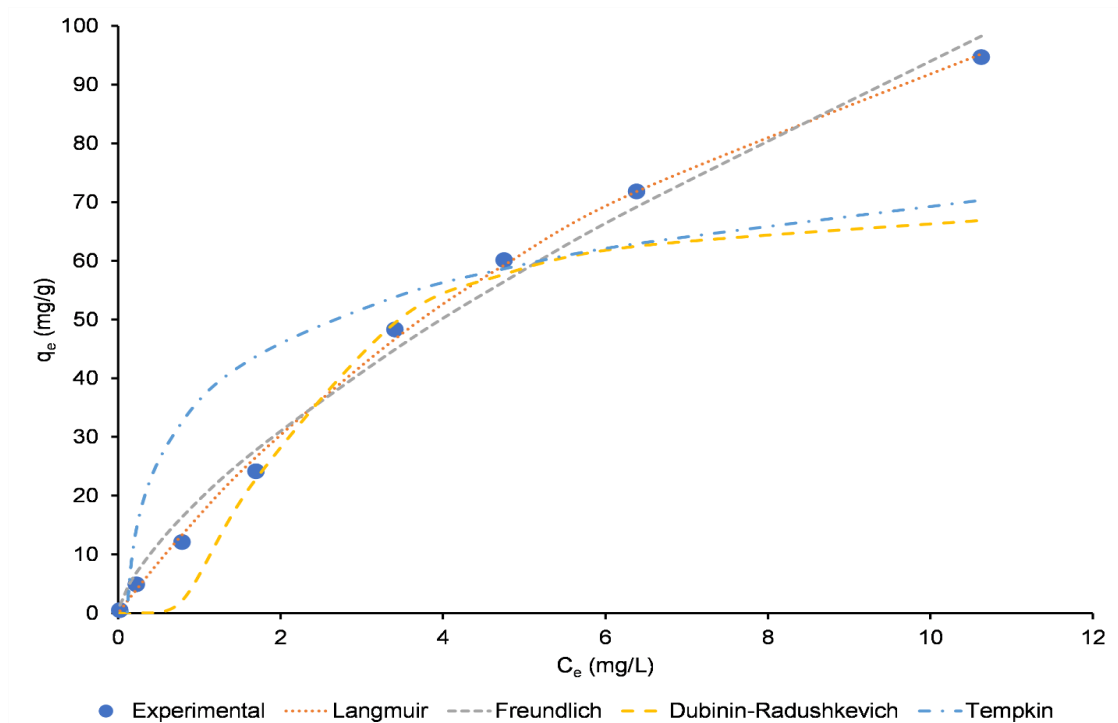
Figure 14: Adsorption isotherm of Langmuir, Freundlich, Dubinin-Radushkevich , and Temkin models for non-linear analysis of Cr(VI)
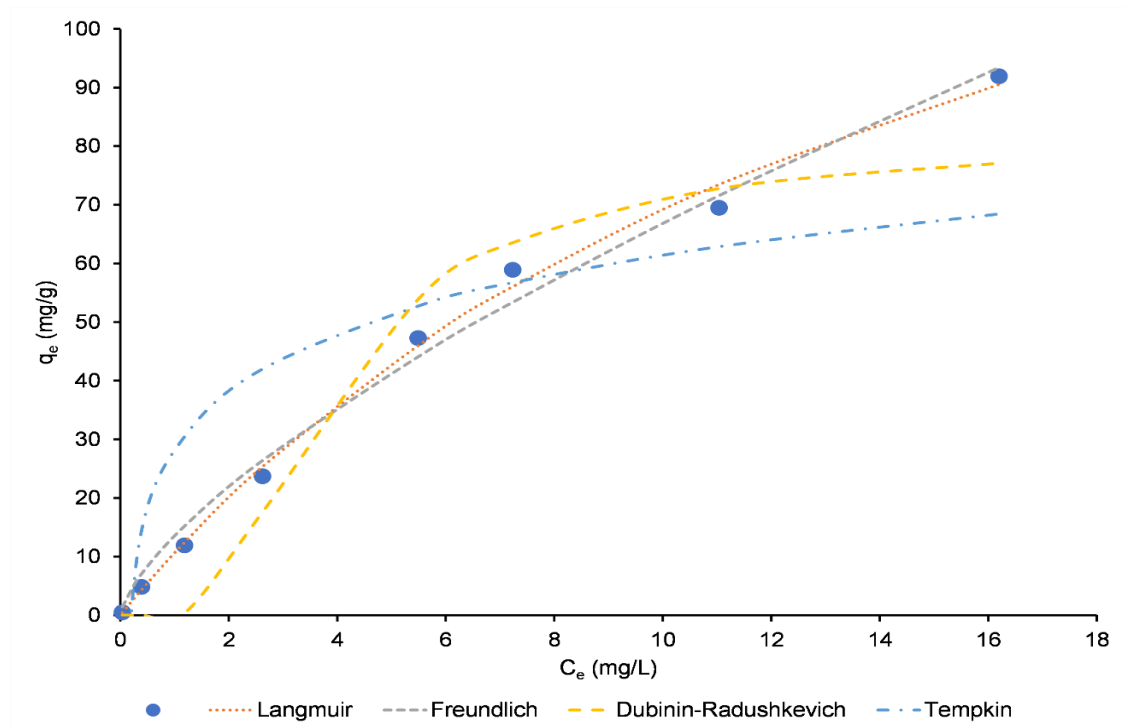
Figure 15: Adsorption isotherm of Langmuir, Freundlich, Dubinin-Radushkevich, and Temkin models for non-linear analysis of Congo red dye.

Table 5: Langmuir, Freundlich, Dubinin-Radushkevich, and Temkin isotherm parameters of Cr(VI) along with correlation coefficient and sum of square error.

	Parameters				
Langmuir	**Qo**	**B**	**R_L**	**R^2**	**SSE**
	186.937	0.098	0.112	0.999	11.883
Freundlich	**K_f**	**n_F**	**$1/n_F$**	**R^2**	**SSE**
	19.312	1.453	0.688	0.991	81.018
Dubinin-Radushkevich	**q_S**	**k_{ad}**		**R^2**	**SSE**
	69.766	8.46E-07		0.938	991.567
Temkin	**A_T**	**b_T**		**R^2**	**SSE**
	12.006	170.954		0.757	2012.709

Table 6: Langmuir, Freundlich, Dubinin-Radushkevich, and Temkin isotherm parameters of Congo red dye along with correlation coefficient and sum of square error.

	Parameters				
Langmuir	**Qo**	**B**	**R_L**	**R^2**	**SSE**
	179.95244	0.0625	0.1621	0.996	30.823
Freundlich	**K_f**	n_F	$^{1/}n_F$	**R^2**	**SSE**
	13.515615	1.440	0.688	0.991	71.35
Dubinin-Radushkevich	q_S	k_{ad}		**R^2**	**SSE**
	81.255	2.39E-06		0.949	490.21
Temkin	**A_T**	**b_T**		**R^2**	**SSE**
	6.8729	170.68		0.77	1791.7

4.3 Analysis of non-linear fitting of the kinetic model

Figure 16 shows the PFO, PSO, PNO and intraparticle diffusion kinetic adsorption model for different concentrations of Cr (VI) by the non-linear method. The rate constant, kinetic parameters, correlation coefficient, and SSE value of each concentration of Cr (VI) used in this study are presented in Table 7. The results show that PNO is the best kinetic model in the present study compared to the other model after analyzing the R^2 and SSE values. The correlation coefficient of PNO (0.999, 0.997, 0.995, 0.994, 0.995, 0.994, 0.995, 0.995) is high and the SEE value is (0.00034-41.26828) low compared to other kinetic models (PFO, PSO, intraarticular diffusion) for various concentrations of chromium (1-200 mg/L). The adsorption capacity value obtained in the PNO kinetic model is 11.908-94.307 mg/g, the rate constant (0.24-0.087) and the n value (1.46-1.31) for the concentration of chromium (1-200 mg/L) on the surface of the algal biochar. Therefore, in the present study, PNO is more suitable for kinetic fitting of parameters that aid in the design of the adsorption process and the determination of the adsorbate (Cr (VI) uptake by the absorbent (algal biochar). Numerous studies have studied and compared the kinetic data of various

adsorption systems using the PFO and PSO equations, but it is not necessary that these equations are always fit for the kinetic model [99, 114, 115]. The result also corresponds to previous research investigating PNO for non-linear regression, is also a good model for studying the kinetics behavior of adsorption [116].
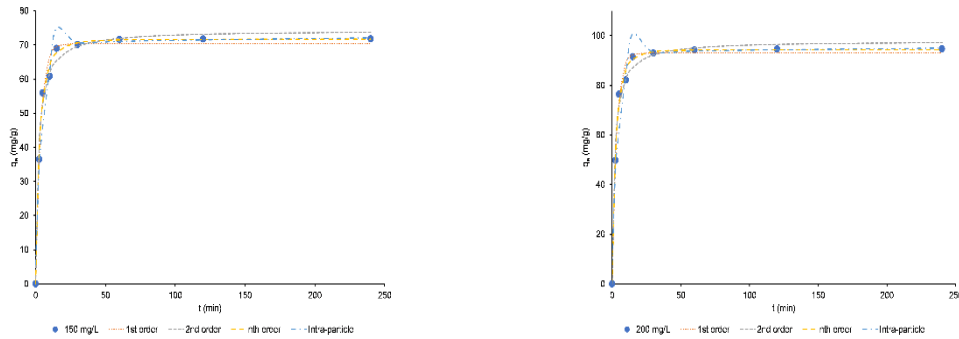
Figure 16: PFO, PSO, PNO and intra-molecular diffusion plots of Cr (VI) removal for (a-h) initial concentration (1-200 mg/L) of Cr (VI) using algal-derived biochar

Table 7: Non-linear analysis of kinetic adsorption parameters for chromium removal by algal-derived biochar

Parameter	Chromium Concentration (mg/L)							
	1	**10**	**25**	**50**	**100**	**125**	**150**	**200**
	Pseudo-first-order equation							
q_e (mg g^{-1})	0.478	4.787	11.908	23.775	47.635	59.394	70.419	93
k_1 (min^{-1})	0.196	0.217	0.242	0.253	0.257	0.269	0.287	0.30
R^2	0.993	0.993	0.991	0.991	0.992	0.991	0.991	0.9
SEE	0.002	0.163	1.216	5.096	18.290	30.864	42.121	61
	Pseudo-second order equation							
q_e (mg g^{-1})	0.511	5.098	12.625	25.181	50.410	62.747	68.321	78
k_2	0.589	0.067	0.031	0.016	0.008	0.007	0.008	0.01

(min^{-1})								
R^2	0.994	0.991	0.989	0.988	0.987	0.986	0.990	0.9
SSE	0.001	0.204	1.542	6.583	28.185	46.119	48.747	96
Pseudo-nth order								
q_e (mg g^{-1})	0.4906	4.881	12.116	24.176	48.329	60.238	71.709	94
k_n	0.242	0.143	0.118	0.098	0.089	0.087	0.066	0.08
n	1.460	1.380	1.362	1.355	1.315	1.315	1.388	1.3
R^2	0.999	0.997	0.995	0.995	0.995	0.994	0.995	0.9
SSE	0.0003	0.071	0.656	2.956	11.373	20.023	22.985	41
Intra-particle diffusion								
k_1	0.116	1.194	3.006	6.021	12.130	15.178	17.889	23
C_1	0.016	0.190	0.649	1.436	2.899	4.000	5.637	8
k_2	0.002	0.019	0.024	0.037	0.058	0.033	0.134	0.1
C_2	0.463	4.633	11.788	23.656	47.5	59	70	92
R^2	0.989	0.985	0.979	0.974	0.974	0.970	0.961	0.95
SSE	0.0025	0.327	2.837	13.768	56.0	98.531	182	387

The result to removal of Congo red Dye is shown in Table 8 which depict that Pseudo nth order is suitable for the kinetics behavior having range is 1.11 -1.31 for 1-200 mg/L concentration. This order is selected due to its more coefficient of determination and less sum of square error as compared to other models. The adsorption isotherm of different kinetics model shown in Figure 17.
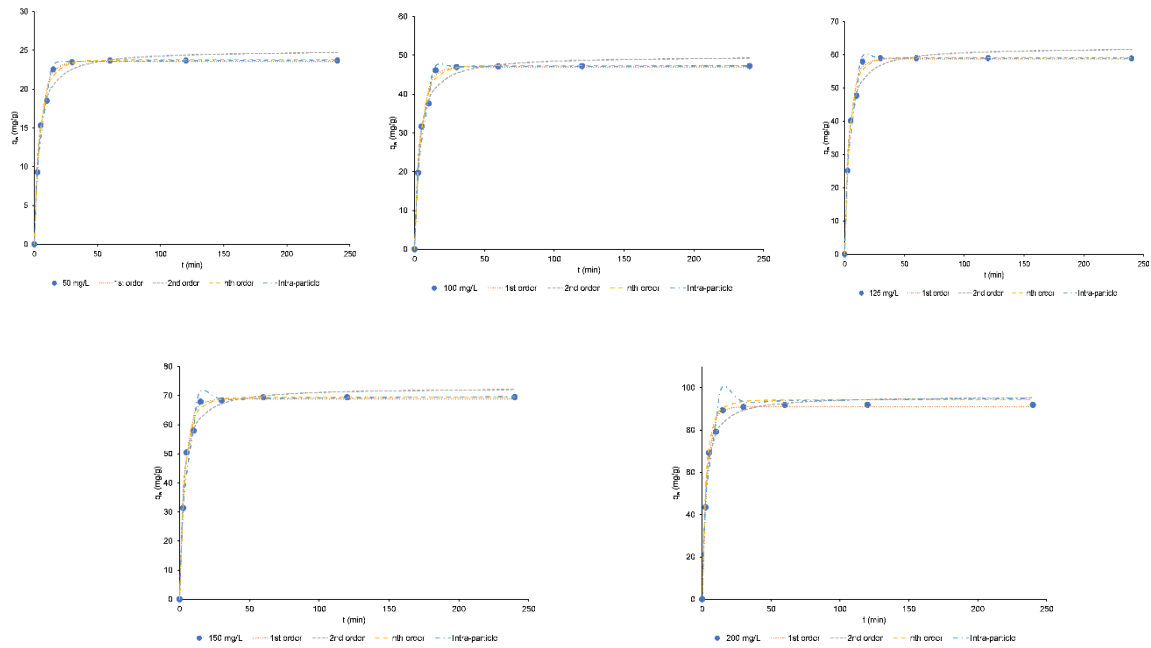
Figure 17:PFO, PSO, PNO and intra-molecular diffusion plots of Congo red dye removal for (a-h) initial concentration (1-200 mg/L) of Congo red dye using algal-derived biochar

Table 8:Non-linear analysis of kinetic adsorption parameters for Congo red dye removal by algal-derived biochar

Parameter	Congo Red Dye Concentration (mg/L)							
	1	**10**	**25**	**50**	**100**	**125**	**150**	**200**
	Pseudo-first-order equation							
q_e (mg g^{-1})	0.476	4.7564	11.814	23.543	47.02	58.78	68	91
k_1 (min^{--1})	0.1497	0.1617	0.1916	0.1916	0.206	0.2136	0.24	0.2
R^2	0.9951	0.9953	0.9948	0.9939	0.992	0.9933	0.9	0.9
SEE	0.00119	0.1099	0.74457	3.4062	16.35	22.84	29	37

	Pseudo-second order equation							
q_e (mg g^{-1})	0.512	5.099	12.623	25.07	49.93	62.35	67	77
k_2 (min^{-1})	0.423	0.047	0.0214	0.0119	0.00659	0.0055	0.04	0.01
R^2	0.982	0.986	0.983	0.984	0.9819	0.9817	0.9	0.9
SSE	0.004	0.330	2.354	8.756	39.704	62.532	71	112
	Pseudo-nth order							
q_e (mg g^{-1})	0.4793	4.804	11.9078	23.76	47.40728	59.222	69	94
k_n	0.1718	0.129	0.1267	0.109	0.1090	0.1145	0.10	0.08
n	1.11	1.207	1.170	1.211	1.191	1.1759	1.2	1.3
R^2	0.9955	0.996	0.995	0.995	0.993	0.994	0.99	0.9
SSE	0.0010	0.078	0.6072	2.5209	13.396	18.843	21.9	153
	Intra-particle diffusion							
k_1	0.1112	1.1405	2.911	5.839	11.8825	14.95	17	95
C_1	0	0	0.0738	0.454477	1.2197	1.7412	3.2	0.07
k_2	0.0017	0.013	0.022	0.017	0.0225	0	0.08	1.5
C_2	0.4576	4.624	11.606	23.462	46.93	58.962	68.3	1.6
R^2	0.990	0.9937	0.9932	0.9925	0.991	0.9904	0.981	0.9
SSE	0.00244	0.14	0.95	4.138	19.33	32.52	86.4	156

4.4 Analysis of ANN for chromium removal

The MLP-based ANN regression model was trained to predict the best model to achieve the target removal efficacy of chromium and congo red dye, as well as the target adsorption kinetic of various concentrations (1-200 mg/L) of Cr (VI) and congo red dye. According to the validation, training, and testing results of the data sets, the one with the highest correlation coefficient and the lowest sum of squared errors was selected. In the present system, 64 data points should be taken for validation. For different times and

concentrations, the structure of the best-performing network was MLP-2-7-1(Cr (VI) and MLP-2-5-1(Congo Red Dye) for both removal efficacy and target adsorption kinetic. MLP-2-7-1 and MLP-2-5-1 mean seven hidden neurons (Cr (VI) and five hidden neurons (Congo Red Dye) and one output neuron with their exponential, logistic and tanh activation function to gain the best correlation coefficient. It is necessary that there be a high correlation coefficient between the model output and the experimental target values to have a good agreement between the results [117]. Figure 18 show the regression plot between the experimental target value of the removal efficacy and the output value of the ANN model. Figure 18 and Fig 19 shows the prediction of the adsorption kinetics of various concentrations of Cr (VI) and Congo red dye for modeling and experimental results with time.
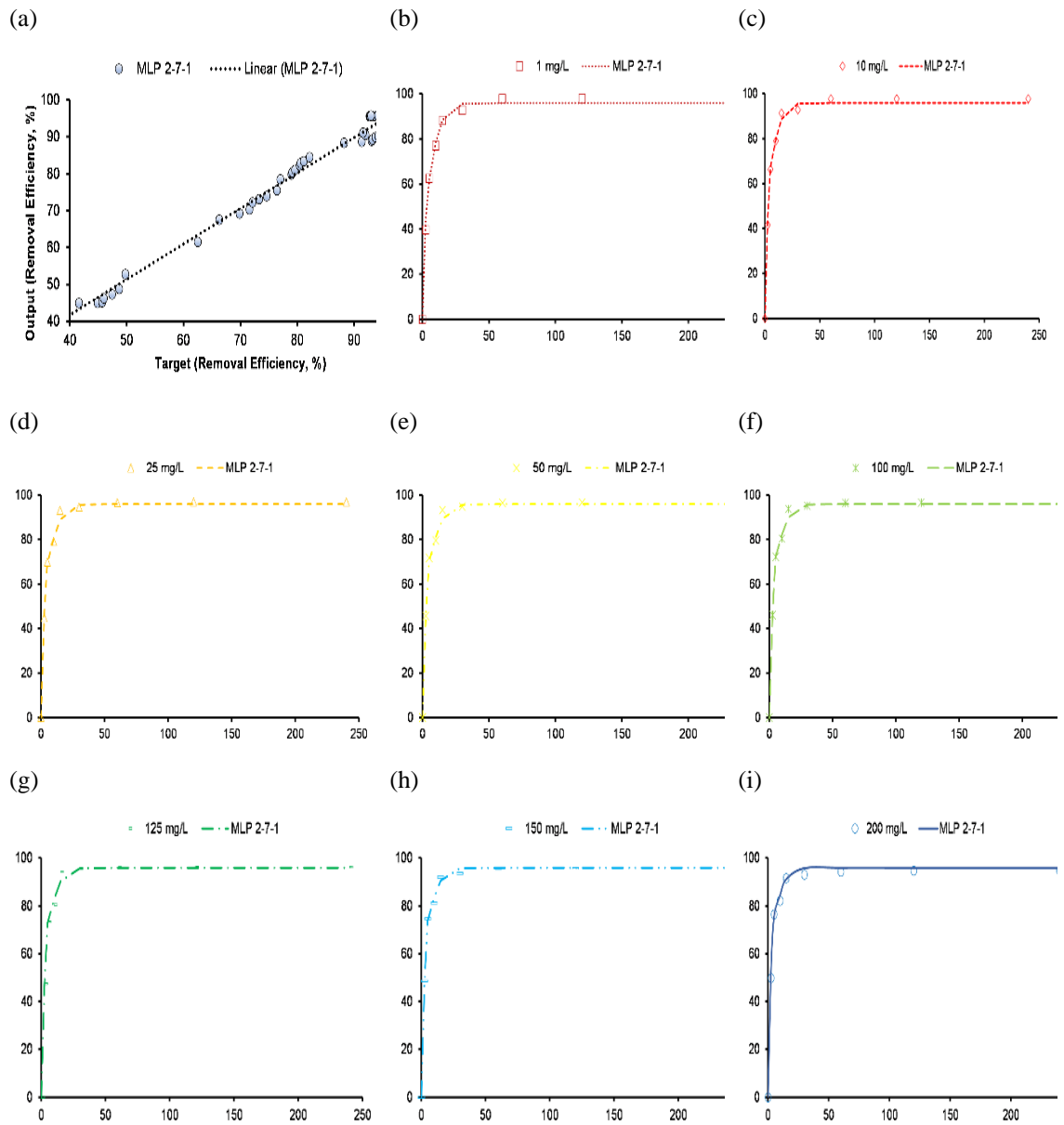
Figure 18(a) Regression plot between the output and target value of Cr (VI) removal; (b)-(i) prediction of Cr (VI) removal for initial concentration (1-200 mg/L) using the ANN model
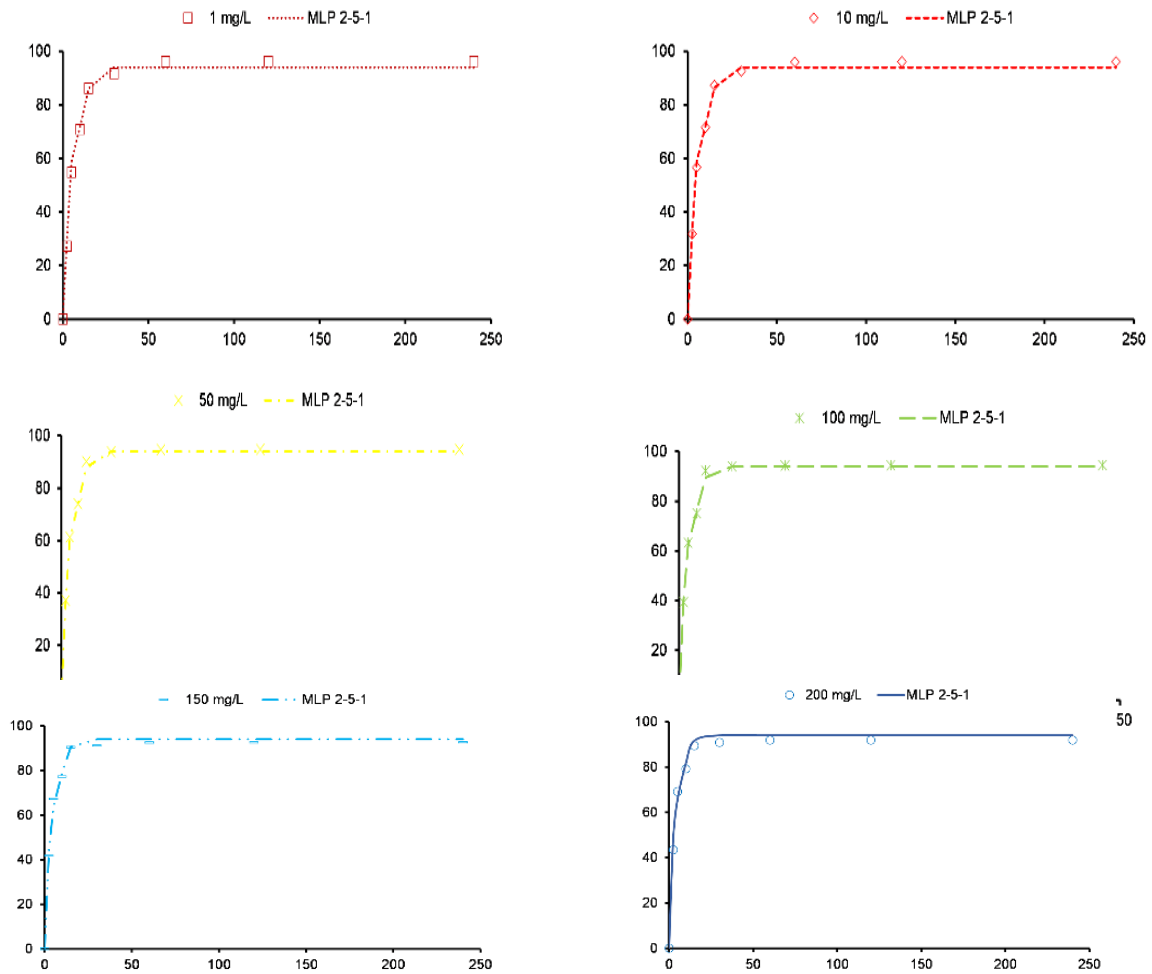
Figure 19 (a) Regression plot between the output and target value of Cr (VI) removal; (b)-(i) prediction of Congo red dye removal for initial concentration (1-200 mg/L) using the ANN model

Table 9 and Table 10 describe the model summary of networks (training, testing, validation (pref. and its error) training algorithm) and model quality. The training prediction was 0.995, the testing prediction (0.996), and the validation preference was (0.997). The result also shows that the testing error (3.564 is more compared to the training and validation error. The training algorithm are BFGS-91 and BFGS-95 which has the capability for very fast convergence and a powerful second-order training algorithm. The number 91 and 95 means that it takes 91 and 95 iterations to converge to reduce the sum

of square error between prediction and experimental value. The model quality name was MLP 2-7-1 and MLP 2-5-1 which illustrates that the absolute mean error with their experimental value is 1.3940 while its adjusted R^2 for SANN is 0.989.

Table 9: Model summary of network (Training, Testing, Validation)

Net. name	Mean Error	Absolute mean error	R squared	Adjusted R squared	Sum of squared error	Valid N
MLP 2-7-1	0.013	1.394	0.989	0.989	214.696	64
MLP 2-5-1	0.086	1.52	0.99	0.99	225.37	64

Table 10: Model quality summary

Net. Name	Test perf.	Validation perf.	Training algorithm	Error function	Hidden activation	Output activation
MLP 2-7-1	0.996	0.997	BFGS 91	SOS	Exponential	Exponential
MLP 2-5-1	0.99	0.99	BFGS 95	SOS	Logistic	Tanh

4.5 Characterization

4.5.1 SEM and EDX analysis

The morphology of the algal and its biochar is analyzed using a scanning electron microscope in Figure 20. The result shows that the algal biomass contains irregular pores with various pore sizes (40.79 nm, 44.72 nm, and 48.66 nm). As we perform pyrolysis of algal biochar at 500 °C temperature, the porosity increases, which confirms the synthesis of biochar. The devolatilization process caused the formation of these pores due to the fast release of volatiles from the algal biomass [118]. The porosity of the algal biochar range is (90-320 nm). The EDX result shows the presence of various cations [119] (Calcium, Potassium, Iron, Zinc etc.) in algal biomass and its biochar. The high porosity and presence of cations help to adsorb Cr (VI) and congo red dye on the surface of algal-derived biochar.
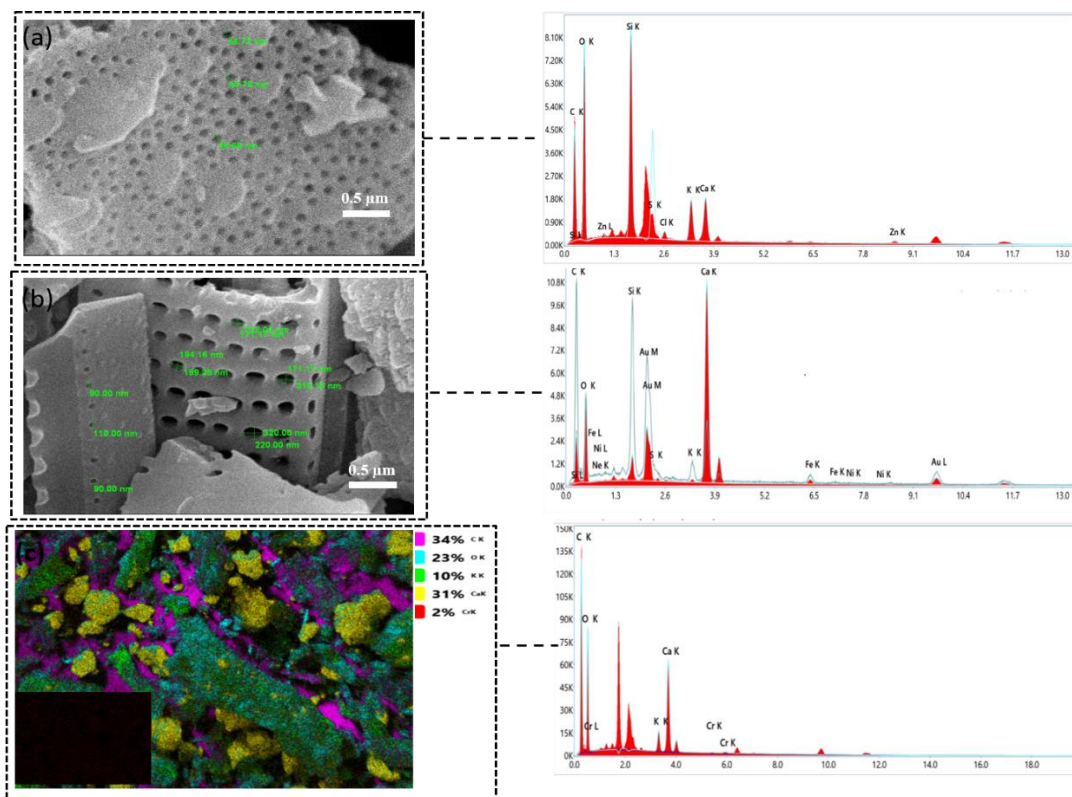
Figure 20: SEM and EDX analysis (a) algae (b) biochar before adsorption (c) after adsorption

4.5.2 FTIR

The FT-IR spectrum is an important characterization technique to detect the functional groups of algae, their derived biochar, and the chromium-loaded algal biochar depicted in Figure 21. The spectra reveal the presence of various functional groups in which a peak around 3356.43 cm^{-1} corresponds to the O–H stretching vibration of the hydroxyl group [61]. A frequency value of 2924.16 cm^{-1} was attributed asymmetric C–H stretching. The value around 2517 cm^{-1} shows the peak of -COOH carboxylic group. The peak around 1801 cm^{-1} was because of -C=0 primary amides and 1648 cm^{-1} indicate the presence of amide [61]. A frequency value of 462 represent the presence of silica. The peak detected at 1093 cm^{-1} can be attributed to the C=O stretching bending and the band at 873 cm^{-1} represent the stretching vibration of C-N, R-O-C, R-O-CH$_3$ and aromatic C-H vibration which consist of protein component in the biomass [120]. The spectra of 706 cm^{-1} shows the -CH$_2$ deformation. The biochar peak shows the shifting of frequency value 3345.43

cm^{-1} to 3424.99 cm^{-1}, 1648 cm^{-1} to 1801 cm^{-1}, and 1093.21 to 1107.95 cm^{-1}. The very weak absorption which was observed at 618.2 cm^{-1} was attributed to the presence of Fe-O bond [121].The peak around 1463 cm-1 represent the presence of -N=N stretching vibration. It is evident that after the adsorption of Cr (VI) and congo red dye on the surface of biochar (500 °C), a small shift in frequency values, indicating the participation of adsorption of Cr (VI) and congo red dye on algae derived biochar (500 °C).
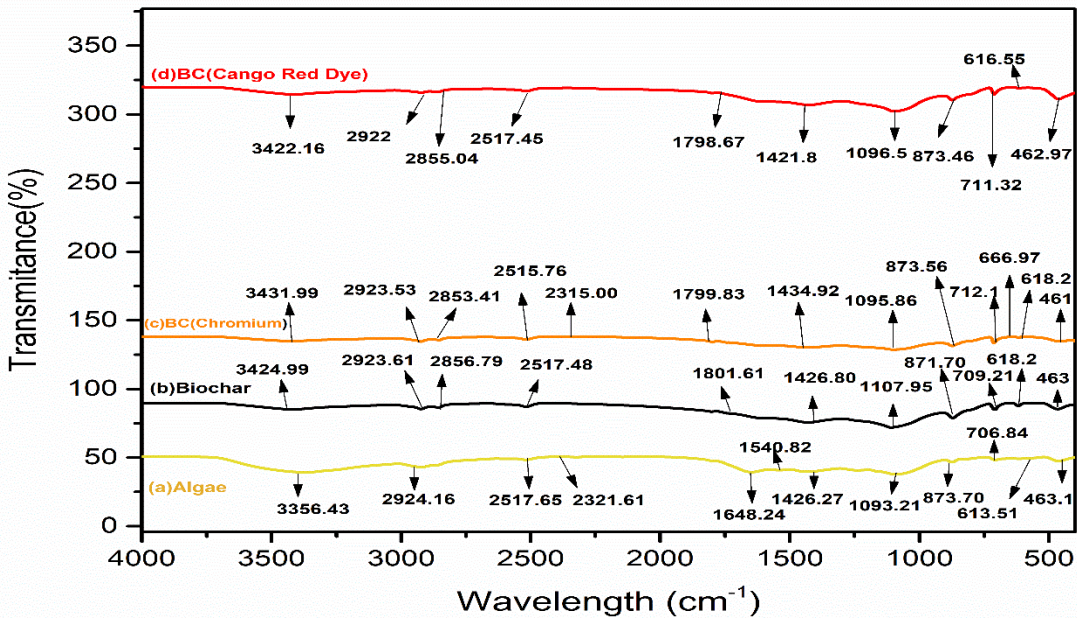
Figure 21: FTIR spectra (a) algae (b) biochar (c) chromium adsorption (d) Congo red dye adsorption

Conclusion

Biochar is an attractive adsorbent for wastewater treatment because of its low cost, high ash content, simple preparation process, and improved physicochemical properties. The study concludes that the yield of biochar obtained from algal biomass through slow pyrolysis is 81.84 % at 500 ℃ with heating rate of 10 ℃/min. The study confirms that biochar has the ability to adsorb Cr (VI) and congo red dye with a maximum removal efficacy of 97.84 % and 96.14% obtained for 1 mg/L concentration at 240 min. The Langmuir adsorption isotherm and the pseudo-nth order kinetic model are fitted models for the adsorption surface of the chromium algal biochar as depicted by non-linear analysis. The analysis is done with the help of coefficient of determination and sum of square error function. This system confirms that the adsorption is monolayer and favorable for chromium removal, as the separation factor value is 0.112. The best model obtained from ANN is M-L-P 2-7-1 and MLP 2-5-1 to attain the target removal efficacy and the kinetic adsorption of chromium and congo red dye removal. This study concludes that the treatment of wastewater for removing chromium and congo red dye through algal biochar helps to attain suitability development.

Recommendation

➢ Biochar is still in the testing stage of research and is not commonly used in general. In underdeveloped countries without entire industrial chains, biochar synthesis and utilization are still rare because of the numerous environmental concerns that cannot be overlooked in the actual application of biochar. More research is required to address potential environmental issues and provide developing countries with relevant research pathways to expand the use of biochar in their countries of origin.

➢ Although biochar can be synthesized from a wide variety of feedstocks (such as wood and agricultural waste), these feedstocks must be ground, washed, and dried before being pyrolyzed to produce the biochar that can be used. In addition, to achieve the optimal sorption effect, additional modifications are required.

➢ Compared to activated carbon, these treatments for biochar are bound to raise production costs. For this reason, future research must find a balance between maximizing biochar's utility and minimizing its production costs.

➢ The growth of algae biomass required for wastewater treatment need a substantial amount of land, water, and nutrients resources.

References

[1] I. Bisschops and H. Spanjers, "Literature review on textile wastewater characterisation," *Environmental Technology,* vol. 24, no. 11, pp. 1399-1411, 2003/11/01 (2003)

[2] N. Bordoloi, R. Goswami, M. Kumar, and R. Kataki, "Biosorption of Co (II) from aqueous solution using algal biochar: kinetics and isotherm studies," *Bioresource technology,* vol. 244, pp. 1465-1469, (2017)

[3] T. Fazal, A. Faisal, A. Mushtaq, A. Hafeez, F. Javed, and A. Alaud Din, "Macroalgae and coal-based biochar as a sustainable bioresource reuse for treatment of textile wastewater. Biomass Convers Biorefinery. 2019," ed.

[4] S. Shabbir, M. Faheem, N. Ali, P. G. Kerr, and Y. Wu, "Periphyton biofilms: A novel and natural biological system for the effective removal of sulphonated azo dye methyl orange by synergistic mechanism," (in eng), *Chemosphere,* vol. 167, pp. 236-246, Jan (2017khan

[5] S.-L. Lim, W.-L. Chu, and S.-M. Phang, "Use of Chlorella vulgaris for bioremediation of textile wastewater," *Bioresource Technology,* vol. 101, no. 19, pp. 7314-7322, 2010/10/01/ (2010)

[6] R. Kant, "Textile dyeing industry an environmental hazard," *Natural Science,* vol. Vol.04No.01, p. 5, (2012), Art no. 17027.

[7] D. Mohan, A. Sarswat, Y. S. Ok, and C. U. Pittman, "Organic and inorganic contaminants removal from water with biochar, a renewable, low cost and sustainable adsorbent – A critical review," *Bioresource Technology,* vol. 160, pp. 191-202, 2014/05/01/ (2014)

[8] M. Bustamante-Torres, D. Romero-Fierro, J. Estrella-Nuñez, S. Pardo, and E. Bucio, "Interaction of Dye Molecules with Fungi: Operational Parameters and Mechanisms," in *Dye Biodegradation, Mechanisms and Techniques: Recent Advances*, S. S. Muthu and A. Khadir Eds. Singapore: Springer Singapore, (2022), pp. 165-191.

[9]   G. Samchetshabam, A. Hussan, T. Gon Choudhury, S. Gita, P. Soholars, and A. Hussan, "Impact of Textile Dyes Waste on Aquatic Environments and its Treatment," 12/01 (2017)

[10]   J. Fito, S. Abrham, and K. Angassa, "Adsorption of Methylene Blue from Textile Industrial Wastewater onto Activated Carbon of Parthenium hysterophorus," *International Journal of Environmental Research,* vol. 14, no. 5, pp. 501-511, 2020/10/01 (2020)

[11]   B. Senthil Rathi and P. Senthil Kumar, "Sustainable approach on the biodegradation of azo dyes: A short review," *Current Opinion in Green and Sustainable Chemistry,* vol. 33, p. 100578, 2022/02/01/ (2022)

[12]   M. Sudha, S. Arul, S. Gopal, and S. Natesan, "Microbial degradation of Azo Dyes: A review," *Int. J. Curr. Microbiol. App. Sci,* vol. 3, pp. 670-690, 01/01 (2014)

[13]   H. Ben Mansour *et al.*, "Acid violet 7 and its biodegradation products induce chromosome aberrations, lipid peroxidation, and cholinesterase inhibition in mouse bone marrow," *Environmental Science and Pollution Research,* vol. 17, no. 7, pp. 1371-1378, 2010/08/01 (2010)

[14]   M. Harja, G. Buema, and D. Bucur, "Recent advances in removal of Congo Red dye by adsorption using an industrial waste," *Scientific Reports,* vol. 12, no. 1, p. 6087, 2022/04/12 (2022)

[15]   M. B. Tahir, M. Sohaib, M. Sagir, and M. Rafique, "Role of Nanotechnology in Photocatalysis," (in eng), *Reference Module in Materials Science and Materials Engineering,* pp. B978-0-12-815732-9.00006-1, (2020)

[16]   S. Velusamy, A. Roy, S. Sundaram, and T. Kumar Mallick, "A Review on Heavy Metal Ions and Containing Dyes Removal Through Graphene Oxide-Based Adsorption Strategies for Textile Wastewater Treatment," *The Chemical Record,* vol. 21, no. 7, pp. 1570-1610, (2021)

[17]   H. Ali, E. Khan, and I. Ilahi, "Environmental Chemistry and Ecotoxicology of Hazardous Heavy Metals: Environmental Persistence, Toxicity, and Bioaccumulation," *Journal of Chemistry,* vol. 2019, p. 6730305, 2019/03/05 (2019)

[18] G. K. Kinuthia, V. Ngure, D. Beti, R. Lugalia, A. Wangila, and L. Kamau, "Levels of heavy metals in wastewater and soil samples from open drainage channels in Nairobi, Kenya: community health implication," (in eng), *Sci Rep,* vol. 10, no. 1, pp. 8434-8434, (2020)

[19] M. Rafati Rahimzadeh, M. Rafati Rahimzadeh, S. Kazemi, and A.-A. Moghadamnia, "Cadmium toxicity and treatment: An update," (in eng), *Caspian journal of internal medicine,* vol. 8, no. 3, pp. 135-145, Summer (2017)

[20] A. HOCAOĞLU-ÖZYİĞİT and B. N. GENÇ, "Cadmium in plants, humans and the environment," *Frontiers in Life Sciences and Related Technologies,* vol. 1, no. 1, pp. 12-21, (2020)

[21] T. M. Chiroma, R. O. Ebewele, and F. K. Hymore, "Heavy Metals in Soils and Vegetables Irrigated with Urban Grey Waste Water in Fagge, Kano, Nigeria," (in eng), *J Environ Sci Eng,* vol. 56, no. 1, pp. 31-6, Jan (2014)

[22] I. I. Ozyigit, I. Dogan, S. Igdelioglu, E. Filiz, S. Karadeniz, and Z. Uzunova, "Screening of damage induced by lead (Pb) in rye (Secale cereale L.) – a genetic and physiological approach," *Biotechnology & Biotechnological Equipment,* vol. 30, no. 3, pp. 489-496, 2016/05/03 (2016)

[23] G. Genchi, A. Carocci, G. Lauria, M. S. Sinicropi, and A. Catalano, "Nickel: Human Health and Environmental Toxicology," *International Journal of Environmental Research and Public Health,* vol. 17, no. 3, p. 679, (2020)

[24] C. C. Alvarez, M. E. Bravo Gómez, and A. Hernández Zavala, "Hexavalent chromium: Regulation and health effects," *Journal of Trace Elements in Medicine and Biology,* vol. 65, p. 126729, 2021/05/01/ (2021)

[25] K. K. Onchoke and S. A. Sasu, "Determination of Hexavalent Chromium (Cr (VI)) concentrations via ion chromatography and UV-Vis spectrophotometry in samples collected from nacogdoches wastewater treatment plant, East Texas (USA)," *Advances in Environmental Chemistry,* vol. 2016, (2016)

[26] N. McCarroll, N. Keshava, J. Chen, G. Akerman, A. Kligerman, and E. Rinde, "An evaluation of the mode of action framework for mutagenic carcinogens case study

II: chromium (VI)," *Environmental and molecular mutagenesis,* vol. 51, no. 2, pp. 89-111, (2010)

[27]   M. Khadem, F. Golbabaei, and A. Rahmani, "Occupational exposure assessment of Chromium (VI): A review of environmental and biological monitoring," *International Journal of Occupational Hygiene,* vol. 9, no. 3, pp. 118-131, (2017)

[28]   M. I. Khan, J. H. Shin, and J. D. Kim, "The promising future of microalgae: current status, challenges, and optimization of a sustainable and renewable industry for biofuels, feed, and other products," *Microbial cell factories,* vol. 17, no. 1, pp. 1-21, (2018)

[29]   W. S. Chai, W. G. Tan, H. S. Halimatul Munawaroh, V. K. Gupta, S.-H. Ho, and P. L. Show, "Multifaceted roles of microalgae in the application of wastewater biotreatment: A review," *Environmental Pollution,* vol. 269, p. 116236, 2021/01/15/ (2021)

[30]   W.-L. Chu and S.-M. Phang, "Biosorption of heavy metals and dyes from industrial effluents by microalgae," in *Microalgae biotechnology for development of biofuel and wastewater treatment*: Springer, (2019), pp. 599-634.

[31]   N. A. Qambrani, M. M. Rahman, S. Won, S. Shim, and C. Ra, "Biochar properties and eco-friendly applications for climate change mitigation, waste management, and wastewater treatment: A review," *Renewable and Sustainable Energy Reviews,* vol. 79, pp. 255-273, 2017/11/01/ (2017)

[32]   O. A. Adeleke *et al.*, "2 - Locally Derived Activated Carbon From Domestic, Agricultural and Industrial Wastes for the Treatment of Palm Oil Mill Effluent," in *Nanotechnology in Water and Wastewater Treatment*, A. Ahsan and A. F. Ismail Eds.: Elsevier, (2019), pp. 35-62.

[33]   F. G. Acién, C. Gómez-Serrano, M. M. Morales-Amaral, J. M. Fernández-Sevilla, and E. Molina-Grima, "Wastewater treatment using microalgae: how realistic a contribution might it be to significant urban wastewater treatment?," *Applied Microbiology and Biotechnology,* vol. 100, no. 21, pp. 9013-9022, 2016/11/01 (2016)

[34] A. T. Ubando, A. D. M. Africa, M. C. Maniquiz-Redillas, A. B. Culaba, W.-H. Chen, and J.-S. Chang, "Microalgal biosorption of heavy metals: A comprehensive bibliometric review," *Journal of Hazardous Materials,* vol. 402, p. 123431, 2021/01/15/ (2021)

[35] S. Zullaikah, A. T. Utomo, M. Yasmin, L. K. Ong, and Y. H. Ju, "9 - Ecofuel conversion technology of inedible lipid feedstocks to renewable fuel," in *Advances in Eco-Fuels for a Sustainable Environment*, K. Azad Ed.: Woodhead Publishing, (2019), pp. 237-276.

[36] H. Kamyab *et al.*, "Improved production of lipid contents by cultivating Chlorella pyrenoidosa in heterogeneous organic substrates," *Clean Technologies and Environmental Policy,* vol. 21, no. 10, pp. 1969-1978, (2019)

[37] W. Farooq *et al.*, "Two-stage cultivation of two Chlorella sp. strains by simultaneous treatment of brewery wastewater and maximizing lipid productivity," *Bioresource Technology,* vol. 132, pp. 230-238, 2013/03/01/ (2013)

[38] V. Matamoros, E. Uggetti, J. García, and J. M. Bayona, "Assessment of the mechanisms involved in the removal of emerging contaminants by microalgae from wastewater: a laboratory scale study," *Journal of hazardous materials,* vol. 301, pp. 197-205, (2016)

[39] Z.-q. Hou, M.-y. Luo, Y.-t. Yang, J.-c. Zhou, L.-c. Liu, and J.-j. Cai, "Algae-based carbons: Design, preparation and recent advances in their use in energy storage, catalysis and adsorption," *New Carbon Materials,* vol. 36, no. 2, pp. 278-303, 2021/04/01/ (2021)

[40] X. Li, C. Wang, J. Tian, J. Liu, and G. Chen, "Comparison of adsorption properties for cadmium removal from aqueous solution by Enteromorpha prolifera biochar modified with different chemical reagents," *Environmental Research,* vol. 186, p. 109502, 2020/07/01/ (2020)

[41] M. A. Vale, A. Ferreira, J. C. M. Pires, and A. L. Gonçalves, "Chapter 17 - CO2 capture using microalgae," in *Advances in Carbon Capture*, M. R. Rahimpour, M. Farsi, and M. A. Makarem Eds.: Woodhead Publishing, (2020), pp. 381-405.

[42]   X. N. Law *et al.*, "Microalgal-based biochar in wastewater remediation: Its synthesis, characterization and applications," *Environmental Research,* vol. 204, p. 111966, 2022/03/01/ (2022)

[43]   S. Pang, "Advances in thermochemical conversion of woody biomass to energy, fuels and chemicals," *Biotechnology Advances,* vol. 37, no. 4, pp. 589-597, 2019/07/01/ (2019)

[44]   X. Miao, Q. Wu, and C. Yang, "Fast pyrolysis of microalgae to produce renewable fuels," *Journal of Analytical and Applied Pyrolysis,* vol. 71, no. 2, pp. 855-863, 2004/06/01/ (2004)

[45]   T. Aysu, N. A. Abd Rahman, and A. Sanna, "Catalytic pyrolysis of Tetraselmis and Isochrysis microalgae by nickel ceria based catalysts for hydrocarbon production," *Energy,* vol. 103, pp. 205-214, 2016/05/15/ (2016)

[46]   L. Jia *et al.*, "Ex Situ Catalytic Pyrolysis of Algal Biomass in a Double Microfixed-Bed Reactor: Catalyst Deactivation and Its Coking Behavior," *Energy & Fuels,* vol. 34, no. 2, pp. 1918-1928, 2020/02/20 (2020)

[47]   H. D. Kawale and N. Kishore, "Production of hydrocarbons from a green algae (Oscillatoria) with exploration of its fuel characteristics over different reaction atmospheres," *Energy,* vol. 178, pp. 344-355, 2019/07/01/ (2019)

[48]   K. L. Yu *et al.*, "Adsorptive removal of cationic methylene blue and anionic Congo red dyes using wet-torrefied microalgal biochar: Equilibrium, kinetic and mechanism modeling," *Environmental Pollution,* vol. 272, p. 115986, 2021/03/01/ (2021)

[49]   Y. Y. Gan *et al.*, "Microwave-assisted wet torrefaction of microalgae under various acids for coproduction of biochar and sugar," *Journal of Cleaner Production,* vol. 253, p. 119944, 2020/04/20/ (2020)

[50]   S. M. Heilmann *et al.*, "Hydrothermal carbonization of microalgae," *Biomass and Bioenergy,* vol. 34, no. 6, pp. 875-882, 2010/06/01/ (2010)

[51]   J. Osayi, S. Iyuke, and S. Ogbeide, "Biocrude Production through Pyrolysis of Used Tyres," *Journal of Catalysts,* vol. 2014, pp. 1-9, 05/15 (2014)

[52] Y. Wang, R. Yin, and R. Liu, "Characterization of biochar from fast pyrolysis and its effect on chemical properties of the tea garden soil," *Journal of Analytical and Applied Pyrolysis,* vol. 110, pp. 375-381, 2014/11/01/ (2014)

[53] W.-J. Liu, H. Jiang, and H.-Q. Yu, "Development of Biochar-Based Functional Materials: Toward a Sustainable Platform Carbon Material," *Chemical Reviews,* vol. 115, no. 22, pp. 12251-12285, 2015/11/25 (2015)

[54] M. Palanisamy, M. Srinivasan, S. Uthandi, S. Karthikeyan, and V. Sivasubramanian, "Bio-char production from micro algal biomass of Chlorella vulgaris," *Phykos,* vol. 47, pp. 99-104, 01/01 (2017)

[55] M. Amin and P. Chetpattananondh, "Biochar from extracted marine Chlorella sp. residue for high efficiency adsorption with ultrasonication to remove Cr(VI), Zn(II) and Ni(II)," *Bioresource Technology,* vol. 289, p. 121578, 2019/10/01/ (2019)

[56] C. D. Venkatachalam, S. R. Ravichandran, and M. Sengottian, "Lignocellulosic and algal biomass for bio-crude production using hydrothermal liquefaction: Conversion techniques, mechanism and process conditions: A review," *Environmental Engineering Research,* vol. 27, no. 1, pp. 200555-0, 2 (2022)

[57] K. L. Yu *et al.*, "Microalgae from wastewater treatment to biochar – Feedstock preparation and conversion technologies," *Energy Conversion and Management,* vol. 150, pp. 1-13, 2017/10/15/ (2017)

[58] L. Peng *et al.*, "Iron improving bio-char derived from microalgae on removal of tetracycline from aqueous system," *Environmental Science and Pollution Research,* vol. 21, no. 12, pp. 7631-7640, (2014)

[59] Y. Y. Gan *et al.*, "Torrefaction of microalgal biochar as potential coal fuel and application as bio-adsorbent," *Energy Conversion and Management,* vol. 165, pp. 152-162, 2018/06/01/ (2018)

[60] Q.-V. Bach, W.-H. Chen, S.-C. Lin, H.-K. Sheen, and J.-S. Chang, "Wet torrefaction of microalga Chlorella vulgaris ESP-31 with microwave-assisted heating," *Energy Conversion and Management,* vol. 141, pp. 163-170, 2017/06/01/ (2017)

[61]   M. I. Bird, C. M. Wurster, P. H. de Paula Silva, A. M. Bass, and R. De Nys, "Algal biochar–production and properties," *Bioresource technology,* vol. 102, no. 2, pp. 1886-1891, (2011)

[62]   K. L. Yu *et al.*, "Recent developments on algal biochar production and characterization," *Bioresource Technology,* vol. 246, pp. 2-11, 2017/12/01/ (2017)

[63]   A. T. Koçer, B. Mutlu, and D. Özçimen, "Investigation of biochar production potential and pyrolysis kinetics characteristics of microalgal biomass," *Biomass Conversion and Biorefinery,* vol. 10, no. 1, pp. 85-94, 2020/03/01 (2020)

[64]   L. Delgadillo-Mirquez, F. Lopes, B. Taidi, and D. Pareau, "Nitrogen and phosphate removal from wastewater with a mixed microalgae and bacteria culture," *Biotechnology Reports,* vol. 11, pp. 18-26, 2016/09/01/ (2016)

[65]   G.-J. Zhou, F.-Q. Peng, L.-J. Zhang, and G.-G. Ying, "Biosorption of zinc and copper from aqueous solutions by two freshwater green microalgae Chlorella pyrenoidosa and Scenedesmus obliquus," *Environmental Science and Pollution Research,* vol. 19, no. 7, pp. 2918-2929, 2012/08/01 (2012)

[66]   G. L. Dotto, J. O. Gonçalves, T. R. S. Cadaval, and L. A. A. Pinto, "Biosorption of phenol onto bionanoparticles from Spirulina sp. LEB 18," *Journal of Colloid and Interface Science,* vol. 407, pp. 450-456, 2013/10/01/ (2013)

[67]   L. Y. Lee, S. Gan, M. S. Yin Tan, S. S. Lim, X. J. Lee, and Y. F. Lam, "Effective removal of Acid Blue 113 dye using overripe Cucumis sativus peel as an eco-friendly biosorbent from agricultural residue," *Journal of Cleaner Production,* vol. 113, pp. 194-203, 2016/02/01/ (2016)

[68]   İ. Tüzün, G. Bayramoğlu, E. Yalçın, G. Başaran, G. Çelik, and M. Y. Arıca, "Equilibrium and kinetic studies on biosorption of Hg(II), Cd(II) and Pb(II) ions onto microalgae Chlamydomonas reinhardtii," *Journal of Environmental Management,* vol. 77, no. 2, pp. 85-92, 2005/10/01/ (2005)

[69]   Y. Nuhoglu, E. Malkoc, A. Gürses, and N. Canpolat, "The removal of Cu(II) from aqueous solutions by Ulothrix zonata," *Bioresource Technology,* vol. 85, no. 3, pp. 331-333, 2002/12/01/ (2002)

[70] M. A. Khalaf, "Biosorption of reactive dye from textile wastewater by non-viable biomass of Aspergillus niger and Spirogyra sp," *Bioresource Technology,* vol. 99, no. 14, pp. 6631-6634, 2008/09/01/ (2008)

[71] A. A. Al-Homaidan, J. A. Alabdullatif, A. A. Al-Hazzani, A. A. Al-Ghanayem, and A. F. Alabbad, "Adsorptive removal of cadmium ions by Spirulina platensis dry biomass," (in eng), *Saudi J Biol Sci,* vol. 22, no. 6, pp. 795-800, Nov (2015)

[72] A. A. Al-Homaidan, A. F. Al-Abbad, A. A. Al-Hazzani, A. A. Al-Ghanayem, and J. A. Alabdullatif, "Lead removal by Spirulina platensis biomass," *International journal of phytoremediation,* vol. 18, no. 2, pp. 184-189, (2016)

[73] J. Y. Chin, L. M. Chng, S. S. Leong, S. P. Yeap, N. H. M. Yasin, and P. Y. Toh, "Removal of Synthetic Dye by Chlorella vulgaris Microalgae as Natural Adsorbent," *Arabian Journal for Science and Engineering,* vol. 45, no. 9, pp. 7385-7395, 2020/09/01 (2020)

[74] C.-Y. Chen, H.-W. Chang, P.-C. Kao, J.-L. Pan, and J.-S. Chang, "Biosorption of cadmium by CO2-fixing microalga Scenedesmus obliquus CNW-N," *Bioresource Technology,* vol. 105, pp. 74-80, 2012/02/01/ (2012)

[75] S. Abbas, M. T. Javed, Q. Ali, H. J. Chaudhary, and M. Rizwan, "Chapter 30 - Alteration of plant physiology by the application of biochar for remediation of organic pollutants," in *Handbook of Bioremediation*, M. Hasanuzzaman and M. N. V. Prasad Eds.: Academic Press, (2021), pp. 475-492.

[76] M. Ghaedi, *Adsorption: Fundamental Processes and Applications*. Academic Press, (2021).

[77] G. Binda, D. Spanu, R. Bettinetti, L. Magagnin, A. Pozzi, and C. Dossi, "Comprehensive comparison of microalgae-derived biochar from different feedstocks: A prospective study for future environmental applications," *Algal Research,* vol. 52, p. 102103, 2020/12/01/ (2020)

[78] C. Ma, Y. Zhao, H. Chen, Y. Liu, R. Huang, and J. Pan, "Biochars derived from by-products of microalgae pyrolysis for sorption of gaseous H2S," *Journal of Environmental Chemical Engineering,* vol. 10, no. 3, p. 107370, 2022/06/01/ (2022)

[79] S. Sutar, P. Patil, and J. Jadhav, "Recent advances in biochar technology for textile dyes wastewater remediation: A review," *Environmental Research,* vol. 209, p. 112841, (2022)

[80] P. Nautiyal, K. Subramanian, and M. Dastidar, "Adsorptive removal of dye using biochar derived from residual algae after in-situ transesterification: alternate use of waste of biodiesel industry," *Journal of environmental management,* vol. 182, pp. 187-197, (2016)

[81] A. T. Tag, G. Duman, S. Ucar, and J. Yanik, "Effects of feedstock type and pyrolysis temperature on potential applications of biochar," *Journal of Analytical and Applied Pyrolysis,* vol. 120, pp. 200-206, 2016/07/01/ (2016)

[82] Y.-K. Choi *et al.*, "Adsorption behavior of tetracycline onto Spirulina sp. (microalgae)-derived biochars produced at different temperatures," *Science of The Total Environment,* vol. 710, p. 136282, 2020/03/25/ (2020)

[83] H. Li, X. Dong, E. B. da Silva, L. M. de Oliveira, Y. Chen, and L. Q. Ma, "Mechanisms of metal sorption by biochars: Biochar characteristics and modifications," *Chemosphere,* vol. 178, pp. 466-478, 2017/07/01/ (2017)

[84] S. Ortiz-Monsalve *et al.*, *Degradation of a Leather-Dye by the Combination of Depolymerised Wood-Chip Biochar Adsorption and Solid-State Fermentation with Trametes Villosa SCS-10*. (2020).

[85] Y. Ge, S. Zhu, J.-S. Chang, C. Jin, and S.-H. Ho, "Immobilization of Hg(II) on high-salinity Spirulina residue-induced biochar from aqueous solutions: Sorption and transformation mechanisms by the dual-mode isotherms," *Environmental Pollution,* vol. 265, p. 115087, 2020/10/01/ (2020)

[86] H. Zheng *et al.*, "Adsorption of p-nitrophenols (PNP) on microalgal biochar: Analysis of high adsorption capacity and mechanism," *Bioresource Technology,* vol. 244, pp. 1456-1464, 2017/11/01/ (2017)

[87] X. Tan, S. Zhu, P. L. Show, H. Qi, and S.-H. Ho, "Sorption of ionized dyes on high-salinity microalgal residue derived biochar: Electron acceptor-donor and metal-organic bridging mechanisms," *Journal of Hazardous Materials,* vol. 393, p. 122435, 2020/07/05/ (2020)

[88]   G. Enaime, A. Baçaoui, A. Yaacoubi, and M. Lübken, "Biochar for Wastewater Treatment—Conversion Technologies and Applications," *Applied Sciences,* vol. 10, no. 10, p. 3492, (2020)

[89]   W.-H. Chen, M.-Y. Huang, J.-S. Chang, and C.-Y. Chen, "Torrefaction operation and optimization of microalga residue for energy densification and utilization," *Applied Energy,* vol. 154, pp. 622-630, 2015/09/15/ (2015)

[90]   Y.-D. Chen, F. Liu, N.-Q. Ren, and S.-H. Ho, "Revolutions in algal biochar for different applications: State-of-the-art techniques and future scenarios," *Chinese Chemical Letters,* vol. 31, no. 10, pp. 2591-2602, 2020/10/01/ (2020)

[91]   Q.-V. Bach and W.-H. Chen, "A comprehensive study on pyrolysis kinetics of microalgal biomass," *Energy conversion and management,* vol. 131, pp. 109-116, (2017)

[92]   A. Villabona-Ortíz, C. Tejada-Tovar, R. Ortega Toro, K. Peña-Romero, and C. Botello-Urbiñez, "Chrome (VI) ion biosorption modelling in a fixed bed column on Dioscorea rotundata hull," *Journal of Water and Land Development,* pp. 202-209, (2022)

[93]   T. Fazal *et al.*, "Macroalgae and coal-based biochar as a sustainable bioresource reuse for treatment of textile wastewater," *Biomass Conversion and Biorefinery,* vol. 11, no. 5, pp. 1491-1506, (2021)

[94]   K. Y. Foo and B. H. Hameed, "Insights into the modeling of adsorption isotherm systems," *Chemical engineering journal,* vol. 156, no. 1, pp. 2-10, (2010)

[95]   W. S. W. Ngah, S. Fatinathan, and N. A. Yosop, "Isotherm and kinetic studies on the adsorption of humic acid onto chitosan-H2SO4 beads," *Desalination,* vol. 272, no. 1-3, pp. 293-300, (2011)

[96]   A. L. Srivastav, P. K. Singh, and Y. C. Sharma, "Synthesis of a novel adsorbent, hydrous bismuth oxide (HBO2) for the removal of fluoride from aqueous solutions," *Desalination and Water Treatment,* vol. 55, no. 3, pp. 604-614, (2015)

[97]   X. Chen, "Modeling of experimental adsorption isotherm data," *information,* vol. 6, no. 1, pp. 14-22, (2015)

[98]   M. M. Dubinin, "The equation of the characteristic curve of activated charcoal," 1947, vol. 55, pp. 327-329,

[99]   R.-L. Tseng, P.-H. Wu, F.-C. Wu, and R.-S. Juang, "A convenient method to determine kinetic parameters of adsorption processes by nonlinear regression of pseudo-nth-order equation," *Chemical Engineering Journal,* vol. 237, pp. 153-161, 2014/02/01/ (2014)

[100]   T. R. Sahoo and B. Prelot, "Chapter 7 - Adsorption processes for the removal of contaminants from wastewater: the perspective role of nanomaterials and nanotechnology," in *Nanomaterials for the Detection and Removal of Wastewater Pollutants*, B. Bonelli, F. S. Freyria, I. Rossetti, and R. Sethi Eds.: Elsevier, (2020), pp. 161-222.

[101]   K. V. Kumar and S. Sivanesan, "Selection of optimum sorption kinetics: comparison of linear and non-linear method," *Journal of hazardous materials,* vol. 134, no. 1-3, pp. 277-279, (2006)

[102]   D. Gusain, V. Srivastava, M. Sillanpää, and Y. C. Sharma, "Kinetics and isotherm study on adsorption of chromium on nano crystalline iron oxide/hydroxide: linear and nonlinear analysis of isotherm and kinetic parameters," *Research on Chemical Intermediates,* vol. 42, no. 9, pp. 7133-7151, (2016)

[103]   J. Wang and X. Guo, "Adsorption kinetic models: Physical meanings, applications, and solving methods," *Journal of Hazardous Materials,* vol. 390, p. 122156, 2020/05/15/ (2020)

[104]   A. Asfaram, M. Ghaedi, A. Goudarzi, and M. Rajabi, "Response surface methodology approach for optimization of simultaneous dye and metal ion ultrasound-assisted adsorption onto Mn doped Fe 3 O 4-NPs loaded on AC: kinetic and isothermal studies," *Dalton Transactions,* vol. 44, no. 33, pp. 14707-14723, (2015)

[105]   A. Altriki, I. Ali, S. Razzak, I. Ahmad, and W. Farooq, "Assessment of CO2 biofixation and bioenergy potential of microalga Gonium pectorale through its biomass pyrolysis, and elucidation of pyrolysis reaction via kinetics modeling and

artificial neural network," *Frontiers in bioengineering and biotechnology,* vol. 10, (2022)

[106] M. Liang, Y. Ding, Q. Zhang, D. Wang, H. Li, and L. Lu, "Removal of aqueous Cr (VI) by magnetic biochar derived from bagasse," *Scientific reports,* vol. 10, no. 1, pp. 1-13, (2020)

[107] B. Choudhary and D. Paul, "Isotherms, kinetics and thermodynamics of hexavalent chromium removal using biochar," *Journal of Environmental Chemical Engineering,* vol. 6, no. 2, pp. 2335-2343, (2018)

[108] A. El-Sikaily, A. E. Nemr, A. Khaled, and O. Abdelwehab, "Removal of toxic chromium from wastewater using green alga Ulva lactuca and its activated carbon," *Journal of Hazardous Materials,* vol. 148, no. 1, pp. 216-228, 2007/09/05/ (2007)

[109] S. S. Mirza *et al.*, "Biosorption of chromium from tannery effluent using carbon-activated algae granules of Chlorella vulgaris and Scenedesmus obliquus," *International Journal of Environmental Science and Technology,* vol. 18, no. 10, pp. 3061-3070, (2021)

[110] E. A. Abdel-Galil, L. M. S. Hussin, and W. M. El-Kenany, "Adsorption of Cr (VI) from aqueous solutions onto activated pomegranate peel waste," *Desalination Water Treat,* vol. 211, pp. 250-266, (2021)

[111] Z. Sheerazi, S. A. Khan, S. A. Chaudhry, and T. A. Khan, "Non-linear modelling of adsorption isotherm and kinetics of chromium (VI) and celestine blue attenuation using a novel poly (curGheibicumin-citric acid)/MnFe2O4 nanocomposite," *Modeling Earth Systems and Environment,* pp. 1-19, (2022)

[112] Y.-J. Zhang, J.-L. Ou, Z.-K. Duan, Z.-J. Xing, and Y. Wang, "Adsorption of Cr (VI) on bamboo bark-based activated carbon in the absence and presence of humic acid," *Colloids and Surfaces A: Physicochemical and Engineering Aspects,* vol. 481, pp. 108-116, (2015)

[113] L. P. Hoang *et al.*, "Cr (VI) removal from aqueous solution using a magnetite snail shell," *Water, Air, & Soil Pollution,* vol. 231, no. 1, pp. 1-13, (2020)

[114] Y. Xiao, J. Azaiez, and J. M. Hill, "Erroneous Application of Pseudo-Second-Order Adsorption Kinetics Model: Ignored Assumptions and Spurious Correlations," *Industrial & Engineering Chemistry Research,* vol. 57, no. 7, pp. 2705-2709, 2018/02/21 (2018)

[115] V. J. P. Vilar, C. M. S. Botelho, and R. A. R. Boaventura, "Chromium and zinc uptake by algae Gelidium and agar extraction algal waste: Kinetics and equilibrium," *Journal of Hazardous Materials,* vol. 149, no. 3, pp. 643-649, (2007)

[116] V. C. Srivastava, M. M. Swamy, I. D. Mall, B. Prasad, and I. M. Mishra, "Adsorptive removal of phenol by bagasse fly ash and activated carbon: equilibrium, kinetics and thermodynamics," *Colloids and surfaces a: physicochemical and engineering aspects,* vol. 272, no. 1-2, pp. 89-104, (2006)

[117] I. Ali *et al.*, "Kinetic and thermodynamic analyses of dried oily sludge pyrolysis," *Journal of the Energy Institute,* vol. 95, pp. 30-40, (2021)

[118] B. Cao *et al.*, "Seaweed-derived biochar with multiple active sites as a heterogeneous catalyst for converting macroalgae into acid-free biooil containing abundant ester and sugar substances," *Fuel,* vol. 285, p. 119164, (2021)

[119] A. A. Khan *et al.*, "Recent progress in microalgae-derived biochar for the treatment of textile industry wastewater," *Chemosphere,* p. 135565, (2022)

[120] K. K. Jaiswal, V. Kumar, M. S. Vlaskin, and M. Nanda, "Impact of glyphosate herbicide stress on metabolic growth and lipid inducement in Chlorella sorokiniana UUIND6 for biodiesel production," *Algal Research,* vol. 51, p. 102071, (2020)

[121] I. Michalak, S. Baśladyńska, J. Mokrzycki, and P. Rutkowski, "Biochar from A Freshwater Macroalga as A Potential Biosorbent for Wastewater Treatment," *Water*, vol. 11, no. 7,